Article

Current Biology

A caste differentiation mutant elucidates the evolution of socially parasitic ants

Highlights

- A mutant ant strain resembles known social parasites without a worker caste
- These parasitic queen-like variants arose directly from a free-living ancestor
- The variants have a mutant supergene that probably causes their queen-like traits
- This suggests that supergenes can underlie the evolution of ant social parasitism

Authors

Waring Trible, Vikram Chandra, Kip D. Lacy, ..., Leonora Olivos-Cisneros, Samuel V. Arsenault, Daniel J.C. Kronauer

Correspondence

bucktrible@g.harvard.edu (W.T.), dkronauer@rockefeller.edu (D.J.C.K.)

In brief

Trible et al. report a variant strain of the clonal raider ant that expresses queen-like traits in individuals that would normally become workers. These obligately parasitic variants have a mutated supergene and arose directly from their free-living parent strain, suggesting a genetic mechanism for the evolution of ant workerless social parasites.

Trible et al., 2023, Current Biology *33*, 1–12
March 27, 2023
https://doi.org/10.1016/j.cub.2023.01.067

CellPress

Please cite this article in press as: Trible et al., A caste differentiation mutant elucidates the evolution of socially parasitic ants, Current Biology (2023), https://doi.org/10.1016/j.cub.2023.01.067

Current Biology

CellPress
OPEN ACCESS

Article

A caste differentiation mutant elucidates the evolution of socially parasitic ants

Waring Trible,[1,2,9,*] Vikram Chandra,[1,3,7] Kip D. Lacy,[1,7] Gina Limón,[1,4] Sean K. McKenzie,[1,5] Leonora Olivos-Cisneros,[1] Samuel V. Arsenault,[2,3] and Daniel J.C. Kronauer[1,6,8,*]

[1]Laboratory of Social Evolution and Behavior, The Rockefeller University, 1230 York Avenue, New York, NY 10065, USA
[2]John Harvard Distinguished Science Fellowship Program, Harvard University, 52 Oxford Street, Cambridge, MA 02138, USA
[3]Department of Organismic and Evolutionary Biology, Harvard University, 52 Oxford Street, Cambridge, MA 02138, USA
[4]Department of Microbiology, New York University School of Medicine, 430 E. 29th Street, New York, NY 10016, USA
[5]Oxford Nanopore Technologies, Oxford OX4 4DQ, UK
[6]Howard Hughes Medical Institute, New York, NY 10065, USA
[7]These authors contributed equally
[8]Twitter: @DanielKronauer
[9]Lead contact
*Correspondence: bucktrible@g.harvard.edu (W.T.), dkronauer@rockefeller.edu (D.J.C.K.)
https://doi.org/10.1016/j.cub.2023.01.067

SUMMARY

Most ant species have two distinct female castes—queens and workers—yet the developmental and genetic mechanisms that produce these alternative phenotypes remain poorly understood. Working with a clonal ant, we discovered a variant strain that expresses queen-like traits in individuals that would normally become workers. The variants show changes in morphology, behavior, and fitness that cause them to rely on workers in wild-type (WT) colonies for survival. Overall, they resemble the queens of many obligately parasitic ants that have evolutionarily lost the worker caste and live inside colonies of closely related hosts. The prevailing theory for the evolution of these workerless social parasites is that they evolve from reproductively isolated populations of facultative intermediates that acquire parasitic phenotypes in a stepwise fashion. However, empirical evidence for such facultative ancestors remains weak, and it is unclear how reproductive isolation could gradually arise in sympatry. In contrast, we isolated these variants just a few generations after they arose within their WT parent colony, implying that the complex phenotype reported here was induced in a single genetic step. This suggests that a single genetic module can decouple the coordinated mechanisms of caste development, allowing an obligately parasitic variant to arise directly from a free-living ancestor. Consistent with this hypothesis, the variants have lost one of the two alleles of a putative supergene that is heterozygous in WTs. These findings provide a plausible explanation for the evolution of ant social parasites and implicate new candidate molecular mechanisms for ant caste differentiation.

INTRODUCTION

Most ant species have two distinct morphological castes: queens and workers (Data S1). The developmental and genetic mechanisms that underpin these alternative phenotypes remain poorly understood.[1,2] However, the study of caste development and evolution is largely limited to candidate genes from traditional model organisms, in part because it is impractical to isolate and characterize naturally occurring caste mutants using sexually reproducing ants.

One of the most extreme forms of caste evolution occurs in the workerless social parasites, which feature a modified and miniaturized queen morphology and the loss of the worker caste (Figures 1A and 1B).[1,3–5] All workerless social parasites are obligate inquilines: they live inside host colonies that they exploit for food, shelter, and brood care, and they possess a suite of derived phenotypes, known as the inquiline syndrome, that facilitate this lifestyle.[5–9] Workerless social parasites exploit the colonies of closely related ants, which they resemble chemically and morphologically. In fact, the initial host of many workerless social parasites may be the free-living forms of their parental populations.[4,10–12] If we assume that complex parasitic phenotypes evolve gradually via genome-wide selection, the close phylogenetic relationship between parasites and their hosts implies that a newly emerging parasite must quickly develop reproductive isolation to evolve into a highly specialized, obligate workerless social parasite.[10,13–16]

In 1971, E.O. Wilson proposed a mechanism for the evolution of workerless social parasites based on the assumption that parasites cannot sympatrically speciate from their host.[10] He argued that facultative parasitism always evolves before obligate parasitism and the loss of the worker caste. Under this scenario, nascent parasites must be able to survive independently from their host/ancestor so that they can speciate in allopatry and then re-encounter the host and evolve into an obligate parasite. Wilsonincorporated Ernst Mayr's views of speciation into his framework, but earlier researchers, including William Morton Wheeler and Charles Darwin, also proposed that obligate ant social parasites

Please cite this article in press as: Trible et al., A caste differentiation mutant elucidates the evolution of socially parasitic ants, Current Biology (2023), https://doi.org/10.1016/j.cub.2023.01.067

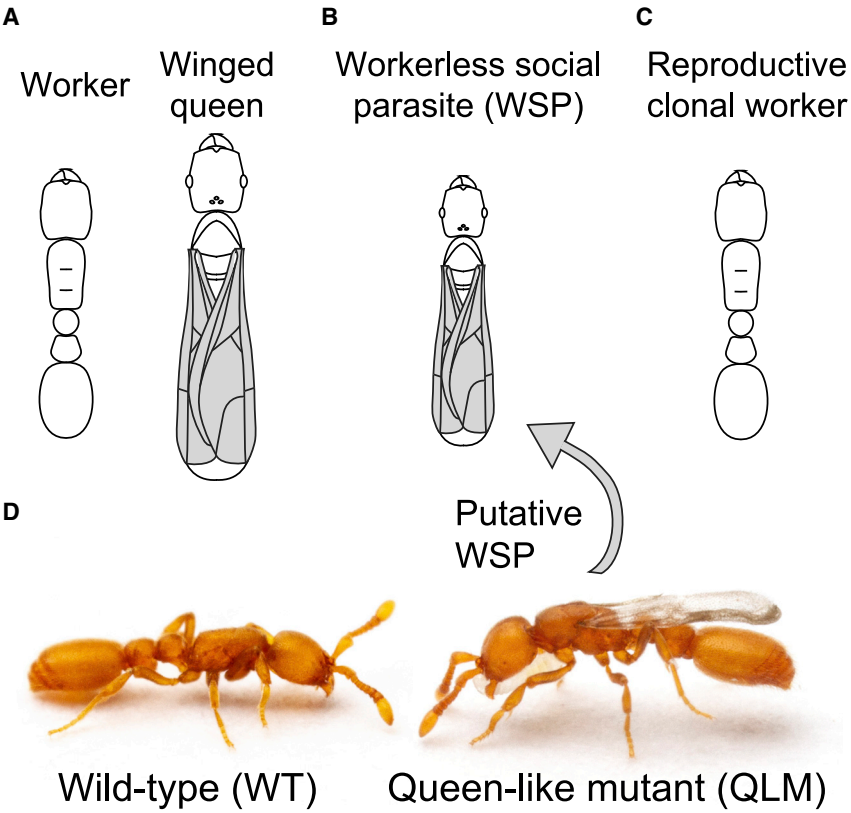

E

Chaperone phenotype	Parent phenotype	# replicate colonies	# wingless ants produced	# winged ants produced
WT	WT	15	149	0
QLM	WT	13	152	0
WT	QLM	12	0	97

Figure 1. A queen-like mutant in the clonal raider ant

(A) Ancestral caste morphology in ants, exemplified by the raider ant *Ooceraea octoantenna*. Relative to workers, queens are larger and possess more developed reproductive, visual, and flight systems.

(B) Workerless social parasite that expresses queen-like morphological features at a worker-like body size, using a miniaturized *O. octoantenna* queen as a hypothetical example.

(C) Caste morphology of WT *O. biroi*. Relative to other *Ooceraea* and the ancestral condition of ants, *O. biroi* has evolutionarily lost the morphological queen caste and instead has colonies that are exclusively composed of parthenogenetic worker ants.

(D) Immature WT *O. biroi* (left) and QLM (right).

(E) Cross-fostering shows that the QLM phenotype is 100% penetrant. Eggs were collected and hatched on glass slides, and colonies were established with 20 adult WTs and 16 young larvae.

Cartoons in (A)–(C) traced from published images.[3] See also Table S1 and Data S1.

evolve from facultative intermediates.[4,10,11] This facultative hypothesis predicts that any obligate parasites should be phylogenetically nested within a clade of facultative parasites, rather than being a sister to a free-living ant. However, recent molecular phylogenetic evidence implies that most workerless social parasites arise directly from free-living ants, rather than evolving from facultative parasites as Wilson's theory proposes.[4]

In recent years, researchers have discovered that many complex intraspecific polymorphisms are conferred by discrete genetic modules, including sex chromosomes, social chromosomes, and other supergenes.[17–25] These discoveries raise the alternative possibility that the suite of traits necessary for workerless social parasitism can be conferred by the inheritance or transformation of a single genetic locus or module.[26] Under this scenario, a workerless social parasite could emerge as an intraspecific genetic variant within a free-living population due to the action of a single locus, while gene flow across the rest of the genome gets disrupted only secondarily. Therefore, the discovery of a pleiotropic genetic module that confers a viable parasitic phenotype could provide a solution to the mystery of the rapid, parallel, and sympatric evolution of ant workerless social parasites.

RESULTS

The clonal raider ant, *Ooceraea biroi*, is a queenless, asexual ant species in which wild-type (WT) individuals have attributes typical of wingless worker ants (Figure 1C).[27] During extensive screening of laboratory colonies, we discovered a series of individuals that possessed prominent wings as pupae and immature adults (Figure 1D). Mature adults shed the wings but retain queen-like wing scars and associated segmentation of the mesosoma (Figure S1). These winged individuals caught our attention because no morphological queens or winged female adults have been reported for this species.[28,29]

To test whether this phenotype arises via genetic variation or phenotypic plasticity, we isolated winged individuals and WT controls for rearing experiments that featured cross-fostering of the two types. Eggs from winged individuals reared by WTs developed into winged individuals with 100% penetrance. In contrast, WT eggs reared by winged individuals invariably developed into WT adults (Figure 1E). Furthermore, a series of randomly selected winged individuals had multilocus microsatellite genotypes identical to those of clonal line A, the WT clonal genotype of the source colony C1 in which the variants were discovered (Table S1).[28] These results indicate that the winged individuals are not products of phenotypic plasticity but represent a genetic variant of clonal line A that, as with workerless

Please cite this article in press as: Trible et al., A caste differentiation mutant elucidates the evolution of socially parasitic ants, Current Biology (2023), https://doi.org/10.1016/j.cub.2023.01.067

CellPress
OPEN ACCESS

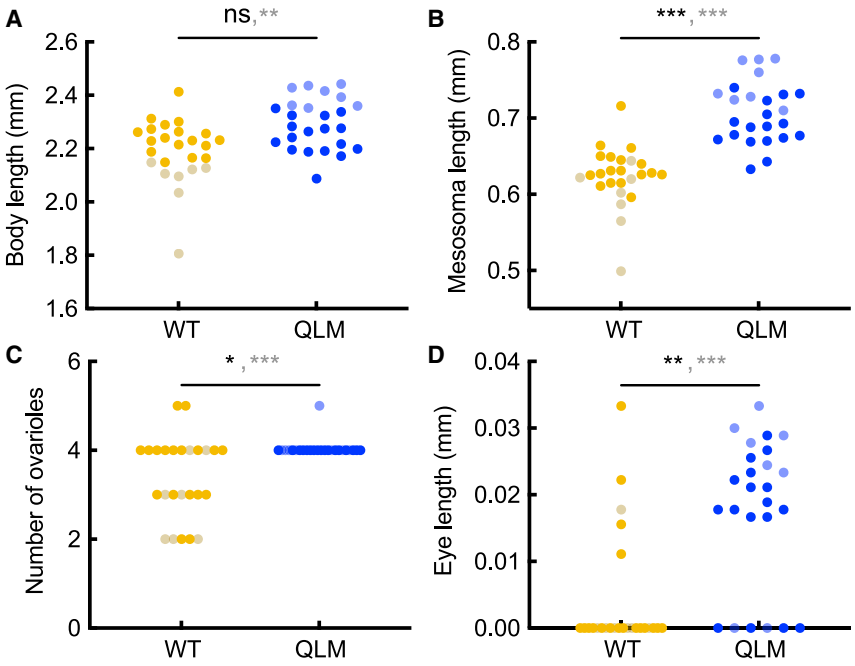

Figure 2. QLMs and WTs overlap in size but differ in caste morphology

(A) Body length of WT and QLM adults. The size distribution of WTs and QLMs is largely overlapping, but QLMs are larger on average.

(B) Mesosoma length of WT and QLM adults. QLMs have a longer mesosoma, reflective of their wing development.

(C) Ovariole number of WT and QLM adults. QLMs have significantly more ovarioles than WTs.

(D) Eye length of WT and QLM adults. QLMs have significantly larger eyes than WTs, most of which lack eyes entirely (Figures S1 and S3). Two p values are reported for each panel: opaque text corresponds to the dataset with individuals excluded to produce a size-matched population (opaque points; n = 18 WT and 17 QLM adults), and translucent text corresponds to the data with all individuals (translucent plus opaque points; n = 25 WT and 25 QLM adults).

Ns, not significant; *p < 0.05; **p < 0.01; ***p < 0.001. p values from unpaired Wilcoxon tests.

See also Figures S1–S3 and Data S2.

social parasites, constitutively develops wings. We therefore designated these ants as a queen-like mutant (QLM) variant.

In principle, there are two developmental genetic mechanisms by which a queen-like morphology could re-appear in a queenless ant species (see Data S1 and Figure S2 for details). In most ant species, morphological caste is an epigenetic outcome of phenotypic plasticity and is tightly coordinated with overall body mass: larger individuals develop wings and a suite of additional queen-like morphological traits, while smaller individuals develop worker-like morphology.[1,5] Some ant lineages display reduced phenotypic plasticity and exhibit a genetic bias for queen development.[30,31] For instance, a "cheater" genotype with queen morphology has been reported from a different queenless clonal ant species (Figure S2).[32] In this and all other previous reports of genetic biases for queen development, the resulting adults are large-bodied and phenotypically indistinguishable from queens induced via phenotypic plasticity, and rare individuals that metamorphose at low body mass develop into adults with typical worker morphology (Data S1; Figure S2). This indicates that the underlying genotypes do not directly induce queen-like differentiation of tissues but instead indirectly induce queen development via an influence on body size (Data S1; Figure S2).[1,3,33] In other words, they affect caste determination (i.e., the probability that a larva will develop into a queen) but do not alter the association between overall body size and adult caste morphology.[1,30,31] This mechanism thus results in phenotypically normal queens that are larger than workers.

The second potential mechanism is inspired by the many workerless social parasites that display queen-like phenotypes at worker-like body sizes (Figure 1B).[5,6,8,9] These phenotypes are distinct from those of typical queens and cannot result directly from changes to the body size distribution (Figure S2). Instead, these workerless social parasites display altered caste differentiation—the allometric scaling mechanisms that coordinate tissue growth with overall body mass.[1,3,8] Therefore, queens produced by genetic changes to caste differentiation should display an abnormal association between body size and adult caste morphology (Figure 1B).[1,3,7,9,34]

To distinguish these alternatives in *O. biroi* QLMs, we collected morphometric data from WTs and QLMs reared under identical conditions (Data S2A). Although the two types show overlap in the distribution of overall body size, QLMs are significantly longer than WTs on average (Figure 2A). QLMs are also queen-like in other features: they have a longer, more segmented mesosoma (Figures 2B, S3A, and S3B), more ovarioles (Figures 2C and S3C), and more developed eyes (Figures 2D and S3D) than WTs.

To test whether QLMs display an altered relationship between body size and caste morphology indicative of a change in caste differentiation, we sub-sampled our initial morphometrics dataset to produce a size-matched population of WT and QLM adults. Although QLMs in this subset do not differ from WTs in body length, they retain significantly greater mesosomal length, ovariole number, and eye length than WTs (opaque dots in Figures 2 and S3A–S3D). These QLMs also have relatively smaller heads and petioles than WTs (Figures S3E and S3F). All of these morphological features have been observed in workerless social parasites (Figure S2).[5,30,31]

To assess morphological similarities between QLMs and the ancestral queen caste of *O. biroi*, we performed a principal components analysis using workers and queens of two close relatives of *O. biroi* that have retained the queen caste, *Ooceraea octoantenna* and *Ooceraea siamensis* (Data S2B and S2C).[35,36] Both *O. octoantenna* and *O. siamensis* queens are larger than the largest workers of their species (Figures 3A and 3B), with queens averaging 22.4% and 15.6% longer than workers, respectively. While *O. biroi* QLMs are only 4.2% longer than WTs, on average (Figures 3A and 3B), a plot of the first two principal components of the morphometric dataset revealed that *O. biroi* QLMs group

Please cite this article in press as: Trible et al., A caste differentiation mutant elucidates the evolution of socially parasitic ants, Current Biology (2023), https://doi.org/10.1016/j.cub.2023.01.067

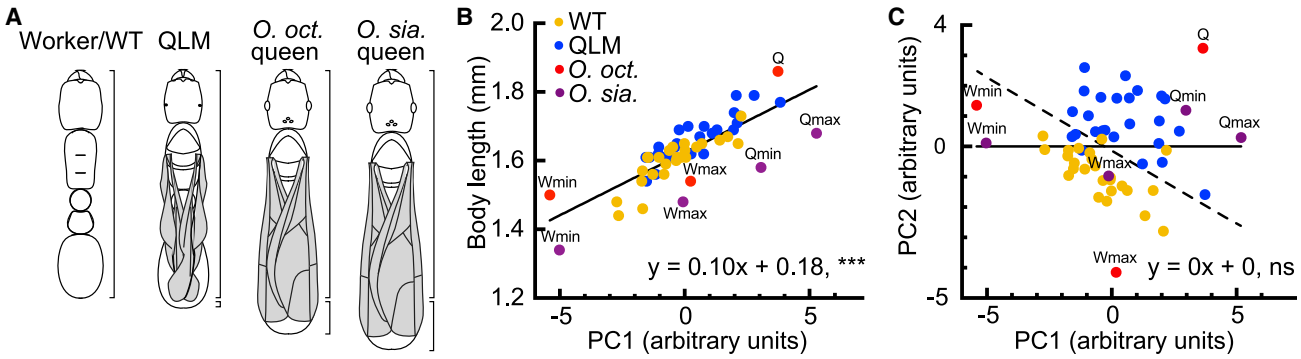

Figure 3. The size overlap between WTs and QLMs is not characteristic of typical *Ooceraea* queens

(A) Cartoons of a QLM, an *O. octoantenna* queen, and an *O. siamensis* queen rescaled to the average worker size of their respective species. QLMs are 4.2% longer than WTs, on average, while *O. octoantenna* and *O. siamensis* queens are 15.6% and 22.4% longer than workers, respectively (lower brackets to the right of each cartoon show the length increase).

(B) Linear regression of PC1 and body length for all samples. Workers of *O. octoantenna* (worker minimum, worker maximum, and one queen) and *O. siamensis* (worker minimum, worker maximum, queen minimum, and queen maximum) have lower body length and PC1 values than queens of their respective species, and workers and queens do not overlap in size. PC1 and body length are correlated, indicating that PC1 is positively associated with body size.

(C) Linear regression of PC1 and PC2 for all samples. A diagonal line (dashed) can separate samples into workers and WTs (lower left) versus queens and QLMs (upper right).

Ns, not significant; ***$p < 0.001$. p values from linear regression with an expected slope of zero. Equations provide best-fit slope and y intercept. *O. sia*, *Ooceraea siamensis*; *O. oct*, *Ooceraea octoantenna*.

See also Figures S1–S3 and Data S2.

with heterospecific queens, while *O. biroi* WTs group with heterospecific workers (Figure 3C). These results confirm that *O. biroi* WTs are homologous to the workers of other *Ooceraea* species and that *Ooceraea* queens are distinctly larger than workers. In contrast, QLMs display a novel morphological syndrome involving queen-like phenotypes at worker-like body size. This indicates that the QLMs do not constitute an atavism that restores the ancestral queen phenotype of *Ooceraea* but instead represent a novel phenotype that resembles the miniature queens of workerless social parasites more closely than any other form of ant natural history variation (Figure S2). Our cross-fostering and morphometric results thus demonstrate that genetic variation in caste differentiation can simultaneously induce worker-sized queens and prevent production of the worker caste.

The morphological worker caste is typically also the specialized behavioral foraging caste in ants, while the morphological queens of free-living and inquiline species are specialized for reproduction and, in most species, do not forage.[37,38] Worker foraging in *O. biroi* takes the form of a multi-step raiding program.[39] Once an *O. biroi* scout worker has encountered prey, it lays a pheromone trail back to the nest, where it recruits a raiding party using a recruitment pheromone. The raiding party then follows the pheromone trail to the prey (Video S1).[39] To test whether QLMs differ from WTs in this behavior, we set up experimental colonies of 16 age-matched ants, composed either of all WTs, all QLMs, or a 50:50 mix of the two variants, and measured multiple aspects of *O. biroi* raiding behavior (Figures 4A–4C). Pure colonies of QLMs conducted a similar number of raids as pure WT colonies, but QLM raiding parties were significantly smaller (mean of 8.75 WT versus 3.87 QLM ants per raid) (Figures 4D and S4A; Videos S1 and S2). In mixed colonies, QLM scouts initiated significantly fewer raids than WT scouts (Figure 4E; WT scouts, 6.75 raids on average; QLM scouts, 1.5 raids on average), and QLMs were under-represented among the ants that participated in the raids (Figure 4F; 29.3%, on average). The genotype of the scout was not associated with the number of ants participating in the raid, implying that the rare QLM scouts show normal recruitment behavior (Figure S4B). These results demonstrate that the underlying genetic factors that produce queen-like morphology also produce a reduced tendency to engage in worker-like foraging behavior.

Lineages that replace workers with worker-sized queens have evolved over a dozen times in ants, suggesting that a wide phylogenetic range of ant species have the capacity to evolve into workerless social parasites.[4] Importantly, every described ant species that has lost the morphological worker caste is an obligate inquiline parasite and typically occurs at a low frequency in the populations of its host.[4] To test whether the QLMs can function as parasites in WT colonies, we collected fitness data at multiple stages of the *O. biroi* life cycle.

Consistent with their elevated ovariole number, QLMs laid approximately twice as many eggs as WTs on average (Figure 5A; 0.43 eggs/QLM/day versus 0.19 eggs/WT/day). Cross-fostering these eggs into matched rearing units revealed that the QLMs exhibit a competitive disadvantage as larvae: their survival to pupation did not differ significantly from WTs when all eggs in the colony were QLMs, but was significantly lower than WT survival in colonies established with 50% WT and 50% QLM eggs (Figure 5B).

While rearing the QLMs, we did not observe any aggression from the WTs but noticed that they frequently died during eclosion. This might be due to the increased difficulty in molting imposed by their bulky wings, as the dead QLMs often had their pupal skin only partially removed. To quantify this effect, we established colonies in which WT adults reared cohorts of pupae that varied in the percentage of QLMs. In colonies with 10% or fewer QLM pupae, survival of QLM pupae was 100% (Figures 5C, S5A, and S5B). In contrast, the survival of QLMs decreased as their frequency increased, with approximately

Please cite this article in press as: Trible et al., A caste differentiation mutant elucidates the evolution of socially parasitic ants, Current Biology (2023), https://doi.org/10.1016/j.cub.2023.01.067

CellPress
OPEN ACCESS

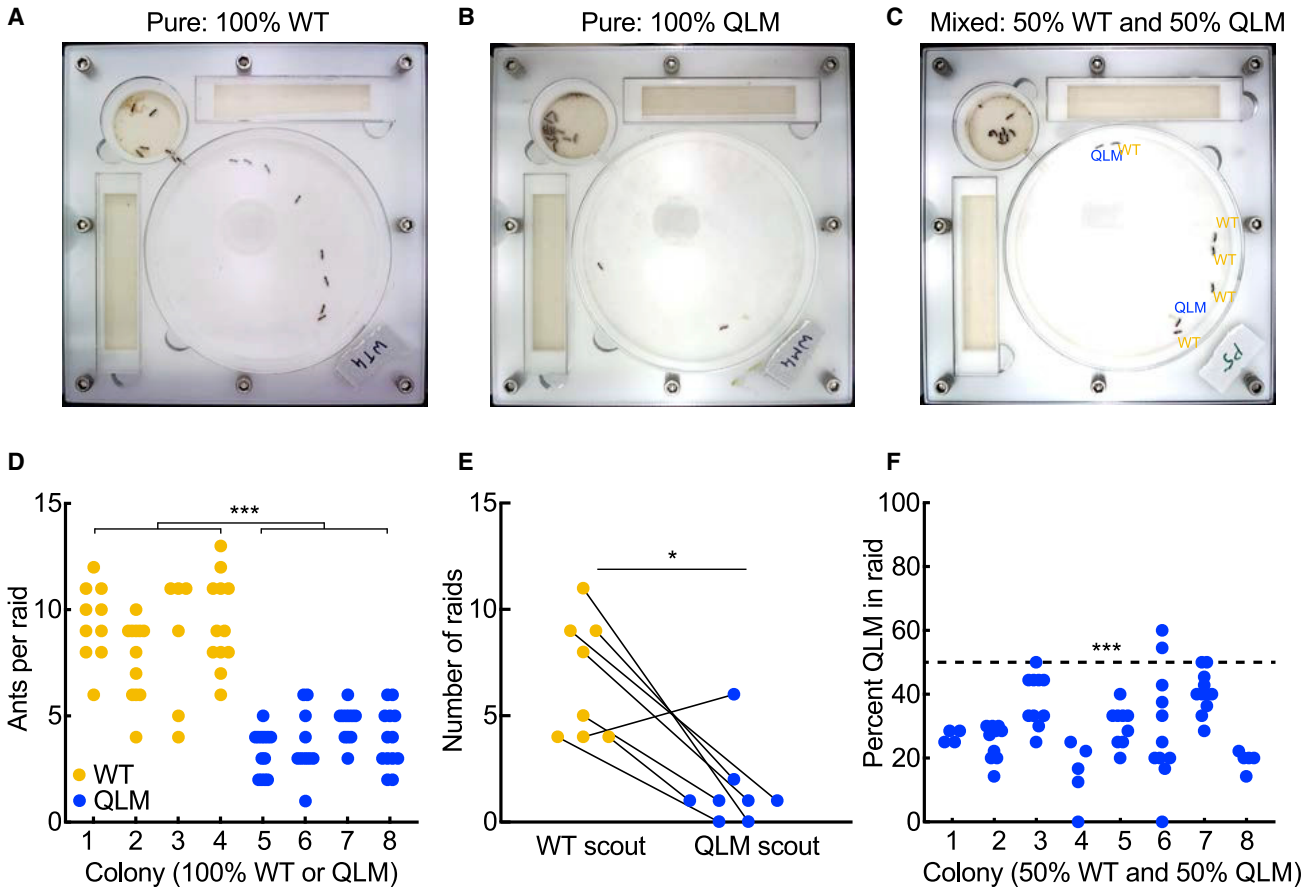

Figure 4. QLMs show a reduced tendency to forage

(A–C) Images taken at peak of raiding activity in representative pure WT (A), pure QLM (B), and mixed (C) colonies (n = 16 ants/colony).

(D) The number of ants per raid in pure WT and QLM colonies (n = 4 colonies composed of 100% WT or 100% QLM adults; n = 40 WT and 47 QLM raids).

(E) The number of raids initiated by WT and QLM scouts in each mixed colony. Lines connect number of WT- and QLM-initiated raids for each of n = 8 colonies composed of 50% WT and 50% QLM adults. A total of 54 and 12 raids were initiated by WT and QLM scouts, respectively.

(F) Fraction of QLMs among raid participants in mixed colonies. Dashed line indicates the null expectation if the two morphs are equally likely to participate in raids.

*$p < 0.05$; ***$p < 0.001$. p values from unpaired (D) or paired (E) two-way Wilcoxon tests or from a one-way Wilcoxon test (F) against an expectation of 50% QLMs in raids.

See also Figure S4 and Videos S1 and S2.

50% survival when more than half of the pupae were QLMs (Figures 5C, S5A, and S5B). The survival of WT pupae was 98.5% and did not vary as a function of the percentage of WT pupae in a colony (Figure S5C). Finally, we studied the ability of QLMs to rear larvae and did not observe any difference in the development time (Figure 5D) or survival (Figure S5D; mean = 80.8% versus 72.7% survival, respectively; p = 0.3184) of WT larvae reared by WT or QLM adults.

These results indicate that QLMs have phenotypes with both positive and negative fitness consequences. In colonies with a minority of QLMs, these fitness effects are balanced such that the proportion of QLMs produced is not significantly different from their frequency in the colony (Figure S5E). In conjunction with our morphometric and behavioral studies, these results show that the QLMs, like workerless social parasites, can function as inquilines of WT colonies.[5,40] The QLMs therefore provide a unique opportunity to investigate the genetic architecture of social parasitism.

To better understand the genetic event that induced the QLM phenotype, we conducted whole-genome short-read resequencing of individual ants at 35× coverage (range: 27.4–41.5) for two QLMs and 15 WT line A adults and used this dataset to create a whole-genome molecular phylogeny (Figure 6A; Data S3A). QLMs are monophyletic and nested within the genetic diversity of colony C1, the colony in which they were discovered (Figure 6A). Given that the species reproduces clonally and that we did not observe any phenotypic intermediates between WTs and QLMs in C1 (or any other colony), this phylogenetic result indicates that the QLMs arose from a WT ancestor due to a recent mutation in a clonal sub-lineage of colony C1.

Mapping the causal genetic basis for this phenotype is challenging because *O. biroi* is parthenogenetic, and we are therefore not able to perform crosses for a traditional association study. However, we can assume that all QLMs have the same genotype at any loci that are causal to the phenotype and that this causal genotype is not found in any WT clonal line A

Please cite this article in press as: Trible et al., A caste differentiation mutant elucidates the evolution of socially parasitic ants, Current Biology (2023), https://doi.org/10.1016/j.cub.2023.01.067

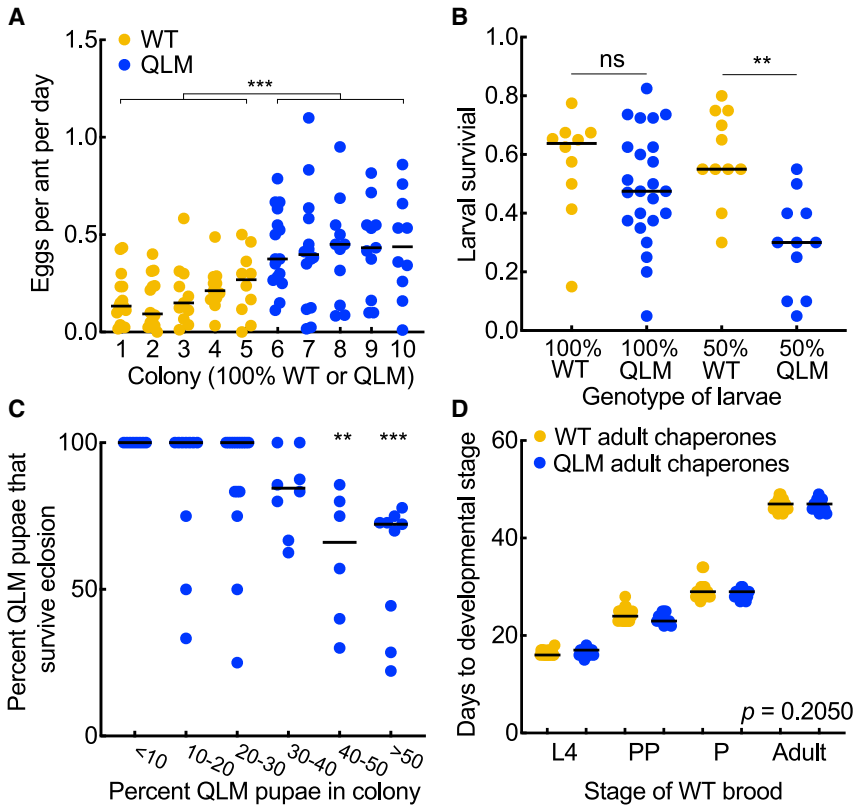

Figure 5. QLMs have both positive and negative shifts in fitness

(A) Egg-laying rate in WT and QLM colonies (n = 5 colonies and 62 paired collection days per genotype).

(B) Egg to pupa survival of brood reared by WT adults (n = 26–40 eggs per colony). Brood were 100% WT (n = 10 colonies), 100% QLM (n = 24 colonies), or 50% WT and 50% QLM (n = 11 colonies; WT and QLM survival are reported separately for each colony).

(C) Percentage of QLMs that survive eclosion (pupa to adult transition). QLMs were reared by WT adults in colonies with varying percentages of QLM versus WT pupae (n = 57 colonies and 6–33 pupae per colony).

(D) Developmental periods for different stages in WT individuals (n = 16 larvae per colony) reared by colonies of WT or QLM adults (n = 19 WT and 13 QLM colonies). L4, 4th larval instar; PP, prepupa; P, pupa. Ns, not significant; $^{**}p < 0.01$; $^{***}p < 0.001$. p values from unpaired (A, comparison of pure WT and QLM colonies in B) or paired (comparison of WT and QLM survival in mixed colonies in B) two-way Wilcoxon tests, or from one-way (C; percent of pupae) or two-way (D; developmental stage and colony type) ANOVA followed by Tukey's test. Black bars depict sample means. In all fitness experiments, colonies consisted of 20 WT or QLM adults.

See also Figure S5.

genomes. Of the 168,819 SNPs in our short-read dataset, only 400 SNPs differed consistently between QLMs and WTs. Interestingly, 364 of these SNPs (91%) were mapped to the second-smallest chromosome in *O. biroi*, chromosome 13 (Figure 6B). Of the SNPs on chromosome 13, all are homozygous in QLMs but heterozygous in WTs. This pattern likely arose via a single, copy-neutral loss of heterozygosity across a segment of the chromosome, which can arise in parthenogenetic organisms that reproduce via post-meiotic fusions due to the inclusion of a recombined and a non-recombined copy of a homologous chromosome in the zygote.[41] Such a loss of heterozygosity can also arise via mitotic recombination, as observed in a substantial portion of human cancers.[42]

The 36 SNPs outside of chromosome 13 that distinguish QLMs from WTs can be ascribed to 28 separate mutations: nine *de novo* SNPs and 19 small losses of heterozygosity (Data S3B). Based on prior estimates from related species, we would expect to see approximately 1.6 *de novo* SNPs across the genome for each generation (assuming a mutation rate of ca. 3.5×10^{-9}/haploid genome/generation[43,44] and a haploid genome size of 224 Mbp in *O. biroi*[45]). The nine *de novo* SNPs that distinguish QLMs from colony C1 WTs therefore imply that the QLMs originated in our lab culture only a few generations ago. In light of this recent origin and the very small number of mutations that distinguish the QLM lineage from WTs (including SNPs, indels, and losses of heterozygosity; Data S3B), it is probable that a single mutational event induced the QLM phenotype rather than that it arose via a gradual series of mutations.

We manually inspected all loci with genotypes unique to QLMs outside of chromosome 13 and did not detect any compelling candidates (Data S3B). Chromosome 13, on the other hand, is unusual in that it is heteromorphic in the *O. biroi* karyotype and contains by far the highest density of contigs in the *O. biroi* genome assembly (Figure 6C).[45,46] Chromosomes with similar features are known to underlie alternative phenotypes in many animals, including sex chromosomes and the supergenes that regulate social organization in multiple species of ants.[24,25,47] Using further bioinformatic characterization, we found that chromosome 13 is enriched for transposable elements and low in proportionate exon content, similar to the fire ant social chromosome and the Y chromosome of *Drosophila melanogaster* (Figures 6D and 6E). These sequence characteristics are found in WT line A ants, implying that the supergene-like features of chromosome 13 were present before the mutational origin of the QLMs. However, we currently cannot determine precisely when or how these features evolved (see discussion).

To determine the location and contents of the loss of heterozygosity, we used a haplotype-aware algorithm to re-assemble published sequencing data with higher contiguity into a diploid assembly, Obir v5.6. We then used alignments of multiple *de novo* assemblies to further improve the assembly of chromosome 13, yielding a final Obir v5.7 assembly (see STAR Methods for details). This resolved chromosome 13 into three large, ordered scaffolds and three unplaced small contigs, compared with 116 contigs unplaced within the chromosome in the previously published assembly, Obir v5.4 (Data S3C).[45] Comparing the primary and secondary contigs of this haplotype-aware

Please cite this article in press as: Trible et al., A caste differentiation mutant elucidates the evolution of socially parasitic ants, Current Biology (2023), https://doi.org/10.1016/j.cub.2023.01.067

CellPress
OPEN ACCESS

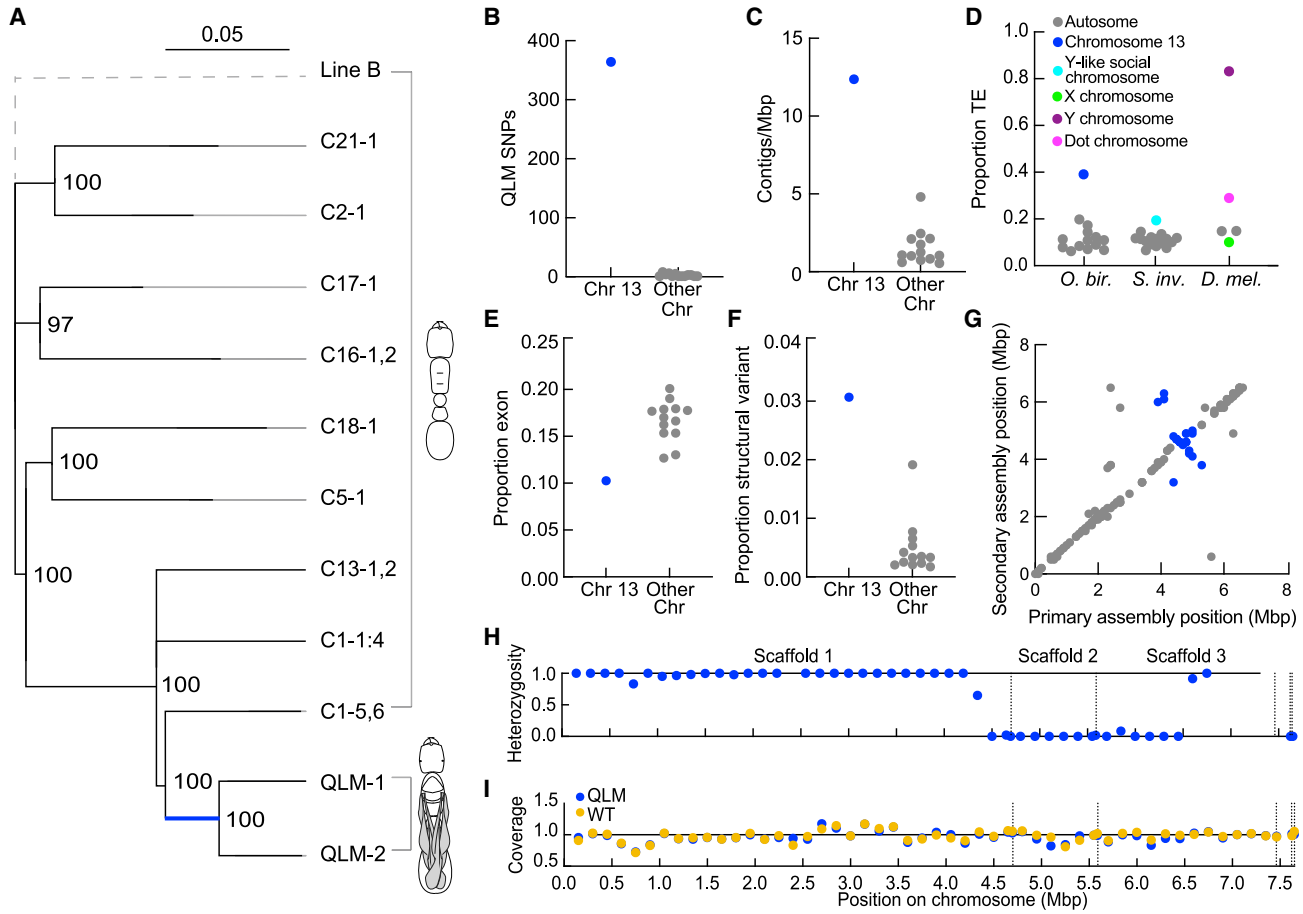

Figure 6. QLMs have a large loss of heterozygosity in a putative supergene

(A) Maximum likelihood phylogeny from whole genomes of 15 WT clonal line A ants and two QLMs, with a single clonal line B ant as an outgroup (gray). Clades of WT ants from the same colony are collapsed. Numbers at nodes represent bootstrap support from 100 replicates, and the scale bar indicates 5% divergence among polymorphic sites across the dataset. Nodes with less than 90% bootstrap support are collapsed.

(B) The number of SNPs distinguishing QLMs from WTs on chromosome 13 versus all other 13 chromosomes. These SNPs correspond to the heavy blue bar on the phylogeny in (A).

(C) Contigs per megabase (Mbp) for *O. biroi* chromosomes.

(D) Proportion TE for chromosomes in three insect species. Chromosome 13 of *O. biroi* has high TE content, similar to the Y-like social chromosome of fire ants and the non-recombining Y chromosome and dot chromosome of fruit flies, but unlike the X chromosome or autosomes.

(E) Proportion exon for *O. biroi* chromosomes.

(F) Proportion structural variant for *O. biroi* chromosomes.

(G) Sequence alignment dot plot of the primary and secondary assemblies of chromosome 13. The contigs of the secondary assembly were scaffolded by aligning them to the primary assembly, so this plot is expected to provide a minimum estimate of any differences in the spatial organization of the chromosome 13 haplotypes. In spite of this, the region from 3.9 to 5.3 Mbp in the primary assembly (blue points) is partially inverted and partially translocated in the secondary assembly.

(H) Relative heterozygosity per 250-kbp window of chromosome 13 in QLMs in our improved chromosome 13 assembly. Heterozygosity is shown as the fraction of heterozygous sites in the WT sister clade (C1–5 and C1–6) that are also heterozygous in QLMs. The few sites at which QLMs apparently retain heterozygosity are likely spurious and arise in instances where reads from duplicate genomic loci were mis-mapped to a single locus in the reference assembly. Windows without data are homozygous in the WTs. Our final chromosome 13 assembly, v5.7, consists of three large scaffolds and three small unplaced contigs (on the right; dotted vertical lines).

(I) Normalized sequencing read depth per 250-kbp window averaged across both QLMs and the two genomes in the WT sister clade (C1–5 and C1–6).

(A)–(F) and (G)–(I) are based on the Obir v5.4 and v5.7 genome assembly, respectively. *O. bir*, *Ooceraea biroi*; *S. inv.*, *Solenopsis invicta*; *D. mel*, *Drosophila melanogaster*.

See also Figure S6 and Data S3.

assembly revealed that chromosome 13 is enriched for structural variants (defined as indels 50 bp or greater in length) and harbors at least one large inversion (Figures 6F and 6G). These results indicate that chromosome 13 contains a putative supergene, similar to the sex chromosomes and social chromosomes that regulate complex phenotypes in many animals.[20,24,25,47]

The loss of heterozygosity in QLMs can be explained by a recombination event spanning 2.25 Mbp of chromosome 13

Please cite this article in press as: Trible et al., A caste differentiation mutant elucidates the evolution of socially parasitic ants, Current Biology (2023), https://doi.org/10.1016/j.cub.2023.01.067

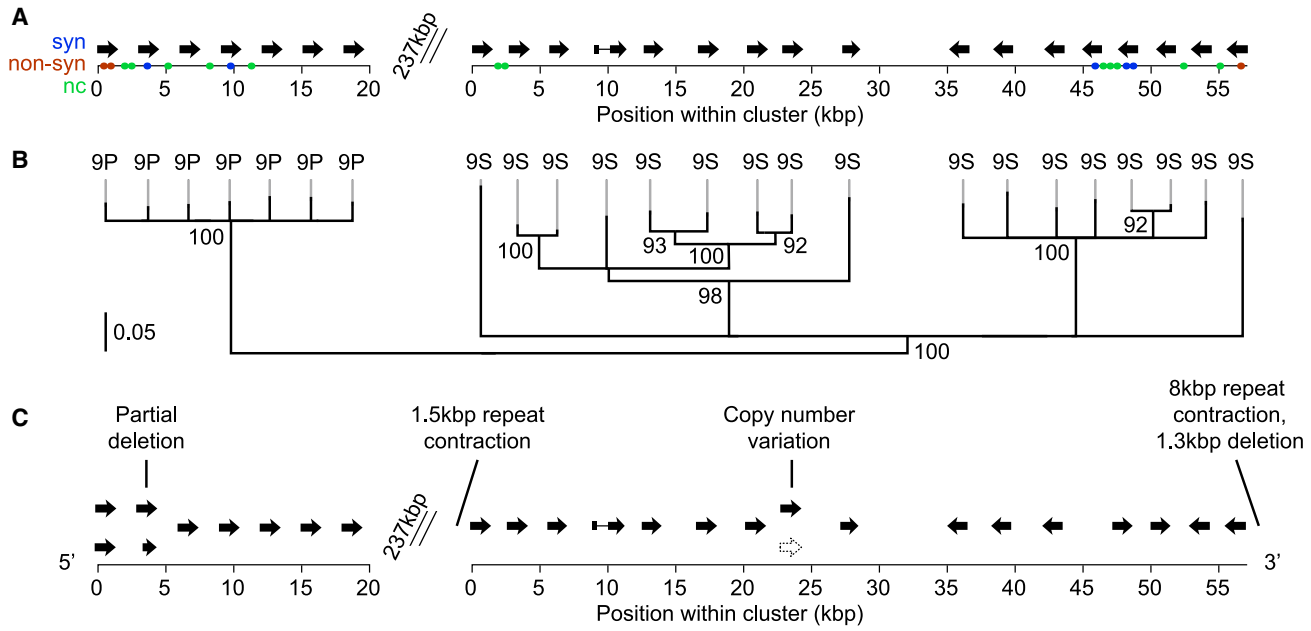

Figure 7. QLMs differ from WTs in two clusters of *CYP9* genes

(A) *CYP9* gene clusters in the Obir v5.4 assembly. Colored dots indicate heterozygosity in WTs in synonymous substitutions (syn), amino acid sequence (non-syn), and non-coding sequence (nc); all of these polymorphisms are homozygous in QLMs (Data S3B). In total, 22 sequence variants are associated with the 24 *CYP9* genes, a significant enrichment relative to the 48 variants affecting the remaining 176 genes in the loss of heterozygosity region ($p < 0.001$, Fisher's exact test) (Data S3F).

(B) The loss of heterozygosity region encodes seven CYP9P and 17 CYP9S proteins (see Figure S7 for identification of gene families within these CYPs). Node labels represent bootstrap support with 100 replicates, and scale bar represents 5% divergence at informative sites. Nodes with less than 90 bootstrap support were collapsed.

(C) Structural variation between haplotypes of the *CYP9* gene clusters, inferred using a *de novo* annotation of the primary and secondary sequence of the Obir v5.6 diploid assembly (Data S3E). The repeat contraction at the 5′ end of the *CYP9S* cluster is 15 kbp from the start codon of the first *CYP9S* gene, while the repeat contraction and deletion at the 3′ end of the array is 8 kbp from the start codon of the final *CYP9S* gene. All of these haplotype differences are heterozygous in WTs but have become homozygous in QLMs.

See also Figure S7, Data S3, and STAR Methods.

(Figure 6H; Data S3C). QLMs do not differ from WTs in sequencing depth within this region, indicating that the homozygosity on chromosome 13 indeed represents a copy neutral loss of heterozygosity rather than a segmental deletion (Figures 6I and S6). At each site in the focal region, the QLM sequence is identical to one of the parent WT haplotypes, showing that it did not accumulate mutations that might contribute to the phenotype subsequent to the recombination event that produced the loss of heterozygosity. We identified the start and stop positions of the loss of heterozygosity but did not find evidence for a loss-of-function mutation caused by the recombination event (Data S3D). The loss of heterozygosity spans 81 structural variants (total length: 98,208 bp) that are heterozygous in WTs and have either become homozygous or have been lost in the QLMs (Data S3E). In light of this large degree of sequence divergence and in conjunction with the fact that supergenes with similar features regulate complex phenotypes in other animals, we hypothesize that the loss of heterozygosity event on chromosome 13 induced the QLM phenotype. However, given that 28 additional mutations elsewhere in the genome also distinguish QLMs from WTs (Data S3B), we cannot formally rule out the possibility that the QLM phenotype was produced by another variant.

The loss of heterozygosity region spans 186 genes in the *O. biroi* genome annotation (Data S3F). Within this gene set, the two most highly enriched GO terms are "oxidoreductase activity" and "metabolic process" (Data S3G), due to a number of *cytochrome P450 9* (*CYP9*) genes (Figure 7). The *CYP9* family is strongly overrepresented in the loss of heterozygosity region ($p = 10^{-20}$, Fisher's exact test using KEGG ortholog groups) (Data S3H). CYPs play essential roles in insect metamorphosis.[48–52] Many uncharacterized insect CYPs are expected to participate in hormone synthesis and metabolism, and ant CYP9s in particular are predicted to bind the molting hormone ecdysone.[52–55] Manual re-annotation showed that the loss of heterozygosity contains 24 of the total 27 *O. biroi CYP9* genes (Figures 7B and S7). The loss of heterozygosity altered the genotype of QLMs relative to WTs in numerous features of the *CYP* array, including amino acid sequences, copy numbers, and adjacent non-coding sequences of *CYPs* (Figures 7A, 7C, and S7; Data S3F). In ants, adult caste phenotypes arise during metamorphosis and are controlled via hormone signaling.[1,2] Thus, the CYP9 enzymes identified here constitute compelling candidate proteins for caste differentiation and other phenotypes of workerless social parasites.

DISCUSSION

Ant queens have fully formed reproductive, visual, and flight systems that are similar to those of their wasp ancestors, while ant

Please cite this article in press as: Trible et al., A caste differentiation mutant elucidates the evolution of socially parasitic ants, Current Biology (2023), https://doi.org/10.1016/j.cub.2023.01.067

workers develop according to a modified program that leads to reduced growth of these tissues during metamorphosis.[1,2,34,56] In other organisms, genetic polymorphisms that reduce or eliminate novel developmental programs (especially alternative phenotypes) are evolutionarily common.[57,58] Early population geneticists assumed that highly pleiotropic genetic variants are generally harmful, but more recent theory suggests that pleiotropic variants, including alleles introgressed via hybridization, can accelerate phenotypic evolution.[22,23,59,60] Our research adds to the evidence that even complex phenotypic syndromes can have a modular genetic and developmental organization that enables rapid evolution.[18,19,61–63]

The QLMs arose from WTs just a few generations before we discovered them in our laboratory colonies. We did not observe any intermediate phenotypes in the source colony, further supporting the conclusion that the QLM phenotype was not gradually assembled across multiple successive generations of clonal evolution. Instead, it seems that the phenotype was induced in a single genetic step: a WT parent produced a daughter with a phenotype resembling that of workerless social parasites. In a sexual ant species, an analogous event could immediately give rise to obligate workerless parasitism without the prior emergence of genome-wide genetic isolation. This raises the possibility that further divergence, including sympatric speciation and morphological, physiological, and behavioral aspects of the inquiline syndrome that are not present in QLMs,[7,9,64] may follow the evolution of obligate parasitism rather than precede it. However, there are many different paths a free-living species can take to become an obligate parasite.[3,4] Our conclusions apply specifically to the evolution of workerless social parasites because QLMs and workerless social parasites share two characteristics that are not found in any other parasitic forms: the loss of the worker caste and a major shift in allometric scaling that produces queens roughly the size of workers in the ancestral population. Other forms of social parasitism, such as brood raiding, nest usurpation, and xenobiosis, are not comparable with workerless social parasites or QLMs.

The QLMs possess a 2.25 Mbp loss of heterozygosity that could have produced the complex QLM phenotype, either by containing a single causal allele or a group of causal alleles in linkage. This loss of heterozygosity is located on chromosome 13, which is structurally similar to the non-recombining social chromosomes of other ant species.[19,62] This suggests the possibility that chromosome 13 contains a supergene that confers social parasitism. Relative to the recent origin of the QLMs, this putative supergene must be ancient and likely segregated in the ancestral sexual population in the form of a recessive Mendelian polymorphism for free-living and workerless social parasite variants. For example, this population could have possessed a recessive *workerless* allele, such that *W/W* and *W/w* are free-living WTs, while *w/w* are QLMs. Line A WTs would then be heterozygous for this supergene (*W/w*), and the loss of heterozygosity produced a variant strain that is homozygous recessive (*w/w*) along some or all of the supergene.

O. biroi is parthenogenetic, so we cannot test for two key features of supergenes: Mendelian inheritance of the QLM phenotype and a suppression of recombination between alternative haplotypes. However, several pieces of evidence support a supergene origin for the QLM phenotype. First, chromosome 13, unlike any other chromosome in the *O. biroi* genome, has characteristics that suggest recombination was suppressed in the ancestral sexual population: a heteromorphic karyotype, at least one large inversion, an enrichment of structural variants and transposable elements (TEs), and a proportional reduction of exons (Figures 6C–6G). Second, the loss of heterozygosity breakpoints do not appear to have affected any protein-coding genes (Data S3D), and all of the variants we identified on chromosome 13 are losses of heterozygosity, suggesting that the phenotype did not result from a *de novo* variant on chromosome 13 in QLMs. Finally, chromosome 13 contains a large array of *CYP9* genes that have many sequence differences between haplotypes (Figure 7A) and may be involved in hormone signaling. However, we cannot definitively prove the supergene hypothesis with the available data, and it is in principle possible that the QLMs were produced via mutations elsewhere in the genome that arose during the clonal evolution of line A.

Regardless of the specific genetic cause, the QLMs demonstrate that a modular genetic architecture can allow an obligate workerless social parasite to emerge within its parental colony and persist for a period of time. This unexpected finding finally provides an empirical solution to the puzzle of workerless social parasite evolution that is consistent with molecular phylogenetic evidence on the evolution of inquilines and growing recognition that supergenes regulate many types of social polymorphisms.[14,15,19,24–26,62]

STAR★METHODS

Detailed methods are provided in the online version of this paper and include the following:

- KEY RESOURCES TABLE
- RESOURCE AVAILABILITY
  - Lead contact
  - Materials availability
  - Data and code availability
- EXPERIMENTAL MODEL AND SUBJECT DETAILS
- METHOD DETAILS
  - Microsatellite and COI sequencing
  - Morphometrics measurements
  - Foraging behavior
  - Fitness measurements
  - Whole-genome sequencing (Illumina)
  - Improved genome assembly
  - Characterization of Chromosome 13
  - Gene-level analysis
- QUANTIFICATION AND STATISTICAL ANALYSIS

SUPPLEMENTAL INFORMATION

Supplemental information can be found online at https://doi.org/10.1016/j.cub.2023.01.067.

ACKNOWLEDGMENTS

Research reported in this publication was supported by the National Institute of General Medical Sciences of the National Institutes of Health under award numbers DP5OD029792 to W.T. and R35GM127007 to D.J.C.K. The content is solely the responsibility of the authors and does not necessarily represent

the official views of the National Institutes of Health. This work was also supported by a John Harvard Distinguished Science Fellowship to W.T. and a Faculty Scholar Award from the Howard Hughes Medical Institute to D.J.C.K. D.J.C.K. is an investigator at the Howard Hughes Medical Institute. We thank Peter Oxley, who rediscovered the queen-like mutants in a laboratory stock colony of *O. biroi* in 2014. We thank Olivier Federigo for generating the initial haplotype-aware genome assembly using the Falcon pipeline and David Nelson for providing the CYP9 subfamily classifications and preliminary enzyme names. Amelia Ritger and Stephany Valdés Rodríguez assisted with ant colony maintenance. Brendan Hunt, Andrew Murray, Naomi Pierce, Ken Ross, Christian Rabeling, and four anonymous reviewers provided feedback on the manuscript. This is Clonal Raider Ant Project Paper #22.

AUTHOR CONTRIBUTIONS

W.T. and D.J.C.K. conceived the project. W.T. and L.O.-C. reared and maintained ants for all experiments. W.T. conducted microsatellite analysis and penetrance experiments. G.L. and W.T. conducted morphometric experiments. V.C. conducted behavioral experiments with help from W.T. and L.O.-C. W.T. performed statistical analyses for morphometric, behavioral, and rearing experiments. K.D.L. conducted DNA extractions for Illumina sequencing, and K.D.L. and W.T. conducted alignment and analysis of Illumina sequence data and characterization of chromosome 13. W.T. conducted DNA extractions for nanopore sequencing, and S.V.A. generated the Flye and Obir v5.7 genome assemblies. S.K.M. generated the Obir v5.6 genome assembly and annotation and assisted with additional genomic analyses. W.T. conducted CYP9 analyses. D.J.C.K. supervised the project. W.T. and D.J.C.K. wrote the paper. All authors discussed the results and approved the final manuscript.

DECLARATION OF INTERESTS

The authors declare no competing interests.

Received: May 31, 2022
Revised: August 31, 2022
Accepted: January 31, 2023
Published: February 28, 2023

REFERENCES

1. Trible, W., and Kronauer, D.J.C. (2021). Hourglass model for developmental evolution of ant castes. Trends Ecol. Evol. *36*, 100–103.
2. Hanna, L., and Abouheif, E. (2021). The origin of wing polyphenism in ants: an eco-evo-devo perspective. Curr. Top. Dev. Biol. *141*, 279–336.
3. Rabeling, C. (2021). Social parasitism. Encycl. Soc. Insects, 836–858.
4. Buschinger, A. (2009). Social parasitism among ants: a review (Hymenoptera: Formicidae). Myrmecol. News *12*, 219–235.
5. Trible, W., and Kronauer, D.J.C. (2017). Caste development and evolution in ants: it's all about size. J. Exp. Biol. *220*, 53–62.
6. Rabeling, C., and Bacci, M. (2010). A new workerless inquiline in the Lower Attini (Hymenoptera: Formicidae), with a discussion of social parasitism in fungus-growing ants. Syst. Entomol. *35*, 379–392.
7. Wilson, E.O. (1984). Tropical social parasites in the ant genus *Pheidole*, with an analysis of the anatomical parasitic syndrome (Hymenoptera: Formicidae). Ins. Soc. *31*, 316–334.
8. Nonacs, P., and Tobin, J.E. (1992). Selfish larvae: development and the evolution of parasitic behavior in the Hymenoptera. Evolution *46*, 1605–1620.
9. Aron, S., Passera, L., and Keller, L. (1999). Evolution of social parasitism in ants: size of sexuals, sex ratio and mechanisms of caste determination. Proc. R. Soc. Lond. B *266*, 173–177.
10. Wilson, E.O. (1971). The Insect Societies (Harvard University Press).
11. Wilson, E.O., and Hölldobler, B. (1990). The Ants (Harvard University Press).
12. Wheeler, W.M. (1910). Ants: Their Structure, Development, and Behavior (Columbia University Press).
13. Buschinger, A. (1990). Sympatric speciation and radiative evolution of socially parasitic ants - heretic hypotheses and their factual background. J. Zoolog. Syst. Evol. *28*, 241–260.
14. Rabeling, C., Schultz, T.R., Pierce, N.E., and Bacci, M. (2014). A social parasite evolved reproductive isolation from its fungus-growing ant host in sympatry. Curr. Biol. *24*, 2047–2052.
15. Buschinger, A. (1986). Evolution of social parasitism in ants. Trends Ecol. Evol. *1*, 155–160.
16. Ward, S. (1996). A new workerless social parasite in the ant genus *Pseudomyrmex* (Hymenoptera: Formicidae), with a discussion of the origin of social parasitism in ants. Syst. Entomol. *21*, 253–263.
17. Ross, K.G., and Keller, L. (1998). Genetic control of social organization in an ant. Proc. Natl. Acad. Sci. USA *95*, 14232–14237.
18. Weber, J.N., Peterson, B.K., and Hoekstra, H.E. (2013). Discrete genetic modules are responsible for complex burrow evolution in *Peromyscus* mice. Nature *493*, 402–405.
19. Purcell, J., Brelsford, A., Wurm, Y., Perrin, N., and Chapuisat, M. (2014). Convergent genetic architecture underlies social organization in ants. Curr. Biol. *24*, 2728–2732.
20. Schwander, T., Libbrecht, R., and Keller, L. (2014). Supergenes and complex phenotypes. Curr. Biol. *24*, R288–R294.
21. Kunte, K., Zhang, W., Tenger-Trolander, A., Palmer, D.H., Martin, A., Reed, R.D., Mullen, S.P., and Kronforst, M.R. (2014). *doublesex* is a mimicry supergene. Nature *507*, 229–232.
22. Orr, H.A. (1998). The population genetics of adaptation: the distribution of factors fixed during adaptive evolution. Evolution *52*, 935–949.
23. Connallon, T., and Hodgins, K.A. (2021). Allen Orr and the genetics of adaptation. Evolution *75*, 2624–2640.
24. Chapuisat, M. (2023). Supergenes as drivers of ant evolution. Myrmecol. News *33*, 1–8.
25. Kay, T., Helleu, Q., and Keller, L. (2022). Iterative evolution of supergene-based social polymorphism in ants. Phil. Trans. R. Soc. B *377*, 20210196.
26. Linksvayer, T.A., Busch, J.W., and Smith, C.R. (2013). Social supergenes of superorganisms: do supergenes play important roles in social evolution? BioEssays *35*, 683–689.
27. Tsuji, K., and Yamauchi, K. (1995). Production of females by parthenogenesis in the ant, *Cerapachys biroi*. Insectes Soc. *42*, 333–336.
28. Kronauer, D.J.C., Pierce, N.E., and Keller, L. (2012). Asexual reproduction in introduced and native populations of the ant *Cerapachys biroi*. Mol. Ecol. *21*, 5221–5235.
29. Trible, W., McKenzie, S.K., and Kronauer, D.J.C. (2020). Globally invasive populations of the clonal raider ant are derived from Bangladesh. Biol. Lett. *16*, 20200105.
30. Schwander, T., Lo, N., Beekman, M., Oldroyd, B.P., and Keller, L. (2010). Nature versus nurture in social insect caste differentiation. Trends Ecol. Evol. *25*, 275–282.
31. Anderson, K.E., Linksvayer, T.A., and Smith, C.R. (2008). The causes and consequences of genetic caste determination in ants (Hymenoptera: Formicidae). Myrmecol. News *11*, 119–132.
32. Tsuji, K., and Dobata, S. (2011). Social cancer and the biology of the clonal ant *Pristomyrmex punctatus* (Hymenoptera: Formicidae). Myrmecol. News *15*, 91–99.
33. Kuhn, A., Darras, H., and Aron, S. (2018). Phenotypic plasticity in an ant with strong caste–genotype association. Biol. Lett. *14*, 20170705.
34. Trible, W., and Kronauer, D.J.C. (2021). Ant caste evo-devo: size predicts caste (almost) perfectly. Trends Ecol. Evol. *36*, 671–673.
35. Bharti, H., Rilta, J.S., and Dhadwal, T. (2021). Two new species of *Ooceraea* (Hymenoptera, Formicidae, Dorylinae) from India with ten-segmented antennae. ZooKeys *1010*, 165–183.
36. Zhou, S.Y., Chen, D.N., and Chen, Z.L. (2020). Discovery of novel *Ooceraea* (Hymenoptera: Formicidae: Dorylinae) species with 8-segmented antennae from China. Sociobiology *67*, 139–143.

37. Brown, M.J.F., and Bonhoeffer, S. (2003). On the evolution of claustral colony founding in ants. Evol. Ecol. Res. *5*, 305–313.

38. Howe, J., Schiøtt, M., and Boomsma, J.J. (2021). Queens of the inquiline social parasite *Acromyrmex insinuator* can join nest-founding queens of its host, the leaf-cutting ant *Acromyrmex echinatior*. Insect. Soc. *68*, 255–260.

39. Chandra, V., Gal, A., and Kronauer, D.J.C. (2021). Colony expansions underlie the evolution of army ant mass raiding. Proc. Natl. Acad. Sci. USA *118*. e2026534118.

40. Brandt, M., Foitzik, S., Fischer-Blass, B., and Heinze, J. (2005). The coevolutionary dynamics of obligate ant social parasite systems - Between prudence and antagonism. Biol. Rev. Camb. Philos. Soc. *80*, 251–267.

41. Engelstädter, J. (2017). Asexual but not clonal: evolutionary processes in automictic populations. Genetics *206*, 993–1009.

42. Zhang, X., and Sjöblom, T. (2021). Targeting loss of heterozygosity: a novel paradigm for cancer therapy. Pharmaceuticals *14*, 1–17.

43. Yang, S., Wang, L., Huang, J., Zhang, X., Yuan, Y., Chen, J.Q., Hurst, L.D., and Tian, D. (2015). Parent-progeny sequencing indicates higher mutation rates in heterozygotes. Nature *523*, 463–467.

44. Liu, H., Jia, Y., Sun, X., Tian, D., Hurst, L.D., and Yang, S. (2017). Direct determination of the mutation rate in the bumblebee reveals evidence for weak recombination-associated mutation and an approximate rate constancy in insects. Mol. Biol. Evol. *34*, 119–130.

45. McKenzie, S.K., and Kronauer, D.J.C. (2018). The genomic architecture and molecular evolution of ant odorant receptors. Genome Res. *28*, 1757–1765.

46. Imai, B.H.T., Urbani, C.B., Kubota, M., Sharma, G.P., Narasimhanna, M.N., Das, B.C., Sharma, A.K., Sharma, A., Deodikar, G.B., Vaidya, V.G., et al. (1984). Karyological survey of Indian ants. Jpn. J. Genet. *59*, 1–32.

47. Furman, B.L.S., Metzger, D.C.H., Darolti, I., Wright, A.E., Sandkam, B.A., Almeida, P., Shu, J.J., and Mank, J.E. (2020). Sex chromosome evolution: so many exceptions to the rules. Genome Biol. Evol. *12*, 750–763.

48. Petryk, A., Warren, J.T., Marqués, G., Jarcho, M.P., Gilbert, L.I., Kahler, J., Parvy, J.P., Li, Y., Dauphin-Villemant, C., and O'Connor, M.B. (2003). Shade is the *Drosophila* P450 enzyme that mediates the hydroxylation of ecdysone to the steroid insect molting hormone 20-hydroxyecdysone. Proc. Natl. Acad. Sci. USA *100*, 13773–13778.

49. Tarver, M.R., Coy, M.R., and Scharf, M.E. (2012). Cyp15F1: a novel cytochrome P450 gene linked to juvenile hormone-dependent caste differention in the termite *Reticulitermes flavipes*. Arch. Insect Biochem. Physiol. *80*, 92–108.

50. Daimon, T., Kozaki, T., Niwa, R., Kobayashi, I., Furuta, K., Namiki, T., Uchino, K., Banno, Y., Katsuma, S., Tamura, T., et al. (2012). Precocious metamorphosis in the juvenile hormone-deficient mutant of the silkworm, *Bombyx mori*. PLOS Genet. *8*, e1002486.

51. Iga, M., and Kataoka, H. (2012). Recent studies on insect hormone metabolic pathways mediated by cytochrome P450 enzymes. Biol. Pharm. Bull. *35*, 838–843.

52. Dermauw, W., Van Leeuwen, T., and Feyereisen, R. (2020). Diversity and evolution of the P450 family in arthropods. Insect Biochem. Mol. Biol. *127*, 103490.

53. Christesen, D., Yang, Y.T., Somers, J., Robin, C., Sztal, T., Batterham, P., and Perry, T. (2017). Transcriptome analysis of *Drosophila melanogaster* third instar larval ring glands points to novel functions and uncovers a cytochrome P450 required for development. G3 (Bethesda) *7*, 467–479.

54. Konorov, E.A., and Belenikin, M.S. (2018). Prediction of the ligands of the CYP9e subfamily of ant cytochrome P450 with the ChEBI ontologies of chemical and biological characteristics. Russ. J. Bioorg. Chem. *44*, 511–517.

55. Ou, Q., Magico, A., and King-Jones, K. (2011). Nuclear receptor DHR4 controls the timing of steroid hormone pulses during Drosophila development. PLOS Biol. *9*, e1001160.

56. Abouheif, E. (2021). Ant caste evo-devo: it's not all about size. Trends Ecol. Evol. *36*, 668–670.

57. Abouheif, E., Favé, M.J., Ibarrarán-Viniegra, A.S., Lesoway, M.P., Rafiqi, A.M., and Rajakumar, R. (2014). Eco-evo-devo: the time has come. In Ecological Genomics: Ecology and the Evolution of Genes and Genomes (Springer), pp. 107–125.

58. West-Eberhard, M.J. (2003). Developmental Plasticity and Evolution (Oxford University Press).

59. Hackinger, S., Kraaijenbrink, T., Xue, Y., Mezzavilla, M., Asan, van Driem, G., Jobling, M.A., de Knijff, P., Tyler-Smith, C., and Ayub, Q. (2016). Wide distribution and altitude correlation of an archaic high-altitude-adaptive EPAS1 haplotype in the Himalayas. Hum. Genet. *135*, 393–402.

60. Zhang, W., Dasmahapatra, K.K., Mallet, J., Moreira, G.R.P., and Kronforst, M.R. (2016). Genome-wide introgression among distantly related Heliconius butterfly species. Genome Biol. *17*, 25.

61. Lamichhaney, S., Fan, G., Widemo, F., Gunnarsson, U., Thalmann, D.S., Hoeppner, M.P., Kerje, S., Gustafson, U., Shi, C., Zhang, H., et al. (2016). Structural genomic changes underlie alternative reproductive strategies in the ruff (*Philomachus pugnax*). Nat. Genet. *48*, 84–88.

62. Wang, J., Wurm, Y., Nipitwattanaphon, M., Riba-Grognuz, O., Huang, Y.C., Shoemaker, D., and Keller, L. (2013). A Y-like social chromosome causes alternative colony organization in fire ants. Nature *493*, 664–668.

63. Todesco, M., Owens, G.L., Bercovich, N., Légaré, J.S., Soudi, S., Burge, D.O., Huang, K., Ostevik, K.L., Drummond, E.B.M., Imerovski, I., et al. (2020). Massive haplotypes underlie ecotypic differentiation in sunflowers. Nature *584*, 602–607.

64. Rabeling, C., Messer, S., Lacau, S., do Nascimento, I.C., Bacci, M., and Delabie, J.H.C. (2019). Acromyrmex fowleri: a new inquiline social parasite species of leaf-cutting ants from South America, with a discussion of social parasite biogeography in the Neotropical region. Insect. Soc. *66*, 435–451.

65. Butler, I.A., Siletti, K., Oxley, P.R., and Kronauer, D.J.C. (2014). Conserved microsatellites in ants enable population genetic and colony pedigree studies across a wide range of species. PLOS One *9*, e107334.

66. Folmer, O., Black, M., Hoeh, W., Lutz, R., and Vrijenhoek, R. (1994). DNA primers for amplification of mitochondrial *cytochrome c oxidase subunit I* from diverse metazoan invertebrates. Mol. Mar. Biol. Biotechnol. *3*, 294–299.

67. Bourne, R. (2010). ImageJ. In Fundamentals of Digital Imaging in Medicine (Springer), pp. 185–188.

68. Van der Auwera, G.A., Carneiro, M.O., Hartl, C., Poplin, R., Del Angel, G., Levy-Moonshine, A., Jordan, T., Shakir, K., Roazen, D., Thibault, J., et al. (2013). From FastQ data to high confidence variant calls: the Genome Analysis Toolkit best practices pipeline. Curr. Protoc. Bioinformatics *43*, 11.10.1–11.10.33.

69. Li, H., Handsaker, B., Wysoker, A., Fennell, T., Ruan, J., Homer, N., Marth, G., Abecasis, G., and Durbin, R.; 1000 Genome Project Data Processing Subgroup (2009). The sequence alignment/map format and SAMtools. Bioinformatics *25*, 2078–2079.

70. Bolger, A.M., Lohse, M., and Usadel, B. (2014). Trimmomatic: A flexible trimmer for Illumina sequence data. Bioinformatics *30*, 2114–2120.

71. Kozlov, A.M., and Stamatakis, A. (2019). Using RAxML-NG in practice. Preprints. https://doi.org/10.20944/preprints201905.0056.v1.

72. Stamatakis, A. (2006). RAxML-VI-HPC: maximum likelihood-based phylogenetic analyses with thousands of taxa and mixed models. Bioinformatics *22*, 2688–2690.

73. Chin, C.S., Peluso, P., Sedlazeck, F.J., Nattestad, M., Concepcion, G.T., Clum, A., Dunn, C., O'Malley, R., Figueroa-Balderas, R., Morales-Cruz, A., et al. (2016). Phased diploid genome assembly with single-molecule real-time sequencing. Nat. Methods *13*, 1050–1054.

74. Kronenberg, Z.N., Rhie, A., Koren, S., Concepcion, G.T., Peluso, P., Munson, K.M., Porubsky, D., Kuhn, K., Mueller, K.A., Low, W.Y., et al. (2021). Extended haplotype-phasing of long-read de novo genome assemblies using Hi-C. Nat. Commun. *12*, 1935.

75. Alonge, M., Soyk, S., Ramakrishnan, S., Wang, X., Goodwin, S., Sedlazeck, F.J., Lippman, Z.B., and Schatz, M.C. (2019). RaGOO: fast and accurate reference-guided scaffolding of draft genomes. Genome Biol. *20*, 224.

76. Darling, A.C.E., Mau, B., Blattner, F.R., and Perna, N.T. (2004). Mauve: multiple alignment of conserved genomic sequence with rearrangements. Genome Res. *14*, 1394–1403.

77. Rissman, A.I., Mau, B., Biehl, B.S., Darling, A.E., Glasner, J.D., and Perna, N.T. (2009). Reordering contigs of draft genomes using the Mauve Aligner. Bioinformatics *25*, 2071–2073.

78. Smit, A.F.A., Hubley, R., and Green, P. (2015), RepeatModeler Open-1.0. http://www.repeatmasker.org.

79. Smit, A.F.A., Hubley, R., and Green, P. (2015), RepeatMasker Open-4.0. http://www.repeatmasker.org.

80. Huerta-Cepas, J., Forslund, K., Coelho, L.P., Szklarczyk, D., Jensen, L.J., Von Mering, C., and Bork, P. (2017). Fast genome-wide functional annotation through orthology assignment by eggNOG-mapper. Mol. Biol. Evol. *34*, 2115–2122.

81. Trible, W., Olivos-Cisneros, L., Mckenzie, S.K., Saragosti, J., Chang, N.C., Matthews, B.J., Oxley, P.R., and Kronauer, D.J.C. (2017). *orco* mutagenesis causes loss of antennal lobe glomeruli and impaired social behavior in ants. Cell *170*, 727–735.e10.

82. Schindelin, J., Arganda-Carreras, I., Frise, E., Kaynig, V., Longair, M., Pietzsch, T., Preibisch, S., Rueden, C., Saalfeld, S., Schmid, B., et al. (2012). Fiji: an open-source platform for biological-image analysis. Nat. Methods *9*, 676–682.

83. McKenna, A., Hanna, M., Banks, E., Sivachenko, A., Cibulskis, K., Kernytsky, A., Garimella, K., Altshuler, D., Gabriel, S., Daly, M., et al. (2010). The Genome Analysis Toolkit: a MapReduce framework for analyzing next-generation DNA sequencing data. Genome Res. *20*, 1297–1303.

84. Li, H. (2013). Aligning sequence reads, clone sequences and assembly contigs with BWA-MEM. https://doi.org/10.48550/arXiv.1303.3997.

85. Mayjonade, B., Gouzy, J., Donnadieu, C., Pouilly, N., Marande, W., Callot, C., Langlade, N., and Muños, S. (2016). Extraction of high-molecular-weight genomic DNA for long-read sequencing of single molecules. BioTechniques *61*, 203–205.

86. Kolmogorov, M., Yuan, J., Lin, Y., and Pevzner, P.A. (2019). Assembly of long, error-prone reads using repeat graphs. Nat. Biotechnol. *37*, 540–546.

Please cite this article in press as: Trible et al., A caste differentiation mutant elucidates the evolution of socially parasitic ants, Current Biology (2023), https://doi.org/10.1016/j.cub.2023.01.067

STAR★METHODS

KEY RESOURCES TABLE

REAGENT or RESOURCE	SOURCE	IDENTIFIER
Critical commercial assays		
QIAamp DNA Micro Kit	QIAGEN	56304
AmpliTaq Gold	Applied Biosystems	4398881
Nextera Flex Library Preparation Kit	Illumina	20060059
NovaSeq SP Flow Cell	Illumina	20027464
Ligation Sequencing Kit	Oxford Nanopore	SQK-LSK109
PromethION Flow Cell	Oxford Nanopore	FLO-PRO002
Deposited data		
De Novo Assemblies & Code	This paper	https://github.com/bucktrible/qlm
Raw Illumina Sequencing Reads	This paper	N/A
Experimental models: Organisms/strains		
Ooceraea biroi Clonal Line A	Kronauer et al.[28]	C1, C2, C5, C13, C16, and C17
Ooceraea biroi Queen-Like Mutant	This paper	N/A
Oligonucleotides		
Microsatellite Primers	Kronauer et al.[28]; Butler et al.[65]	DK371, ES177, D8Z0W, D8M16, D4XW2, ER4IH
LCO: 5'- GGTCAACAAATCAT AAAGATATTGG-3'	Folmer et al.[66]	IDT: LCO
HCO: 5'-TAAACTTCAGGGT GACCAAAAAATCA-3'	Folmer et al.[66]	IDT: HCO
Software and algorithms		
PeakScanner	Applied Biosystems	v1.0
ImageJ	Schneider et al.[67]	https://imagej.nih.gov/ij/download.html
GATK	Van der Auwera et al.[68]	https://gatk.broadinstitute.org/hc/en-us
SAMtools	Li et al.[69]	http://www.htslib.org/download/
Trimmomatic v 0.36	Bolger et al.[70]	https://github.com/usadellab/Trimmomatic
RaxML	Kozlov and Stamatakis[71]; Stamatakis[72]	https://github.com/stamatak/standard-RAxML
Python3	Python Software foundation	https://www.python.org/psf/
GraphPad Prism	GraphPad Prism	Prism v7
R	R Core Team	http://www.R-project.org/
GO+KEGG.Rmd	This paper	N/A
qlm_LOH.Rmd	This paper	N/A
Falcon-Unzip	Chin et al.[73]	https://pb-falcon.readthedocs.io/en/latest/about.html
Falcon-Phase	Kronenberg et al.[74]	https://github.com/phasegenomics/FALCON-Phase
RaGOO	Alonge et al.[75]	https://github.com/malonge/RaGOO
Mauve (Snapshot 2015-02-25)	Darling et al.[76]; Rissman et al.[77]	http://darlinglab.org/mauve/
RepeatModeler	Smit et al.[78]	http://www.repeatmasker.org/
RepeatMasker	Smit et al.[79]	http://www.repeatmasker.org/
topGO	R package, Alexa and Rahnenfuhrer	https://bioconductor.org/packages/release/bioc/html/topGO.html
Eggnog-Mapper	Huerta-Cepas[80]	http://eggnog5.embl.de
Kyoto Encyclopedia of Genes and Genomes (KEGG)	KAAS: an automatic genome annotation and pathway reconstruction server	https://www.genome.jp/kegg/
Prism 7	Graphpad Software	https://www.graphpad.com/scientific-software/prism/

Please cite this article in press as: Trible et al., A caste differentiation mutant elucidates the evolution of socially parasitic ants, Current Biology (2023), https://doi.org/10.1016/j.cub.2023.01.067

RESOURCE AVAILABILITY

Lead contact

Further information and requests for resources and reagents should be directed to and will be fulfilled by the lead contact, Waring Trible (bucktrible@g.harvard.edu).

Materials availability

This study did not generate new unique reagents. All biological materials other than ants are commercially available, and ants can be provided on request, in accordance with federal regulations.

Data and code availability

- Raw morphometric data are available in Data S2.
- Raw Illumina sequencing reads are available at the National Center for Biotechnology Information Short Reads Archive, BioProject PRJNA923657.
- *De novo* genome assemblies (Obir v5.6, Obir v5.7, WT Flye, and QLM Flye) are available at Dryad:dryad.dbrv15f5b.
- Original code is available at https://github.com/bucktrible/qlm.
- Any additional information required to reanalyze the data reported in this paper is available from the lead contact upon request.

EXPERIMENTAL MODEL AND SUBJECT DETAILS

Ooceraea biroi colonies were reared as reported previously.[81] Briefly, colonies were maintained at 25°C in circular Petri dishes (50 mm diameter, 9 mm height) with a plaster of Paris floor ca. 4 mm thick. Colonies were fed 3 times weekly with fire ant (*Solenopsis invicta*) brood and cleaned and watered at least once per week. In the context of this manuscript, wild-type (WT) always refers to phenotypically normal ants derived from Clonal Line A of *O. biroi*.[28] For penetrance and larval survival, colonies of 100% WT or 100% QLM adults (assessed by phenotype) were established without brood. Eggs were removed, allowed to hatch into larvae on glass slides, and then fostered into units to be reared by 16 WT or 16 QLM adults (also referred to as chaperones).

METHOD DETAILS

Microsatellite and COI sequencing

PCR amplification of *cytochrome oxidase I* (COI) was performed using primers as reported previously.[28] Amplification was performed in a final volume of 12 μL using Applied Biosystems' AmpliTaq Gold Kit following manufacturers' recommendations. Cycling profiles started with a denaturation at 94°C for 10 min, and then proceeded with 40 cycles of 94°C for 30 s, 55°C annealing for 30s, 72°C extension for 30 s, finally followed by an extension of 72°C for 10 min. Microsatellite reagents and cycling profiles followed a previous report.[28] Fragment analysis was performed by GeneWiz (Frederick, MD). Microsatellite loci were scored using Peak Scanner (Applied Biosystems).

Morphometrics measurements

Individual ants were dissected to count ovarioles, and then mounted and imaged. Linear measurements were taken using the Fiji distribution of ImageJ.[82] Fifteen measures were used for morphometric analysis, extracted from side view, top view, and head view images. Side view measures were: eye length, head length, head height, Weber's length, mesosoma height, and length of 1st gastral segment (Figure S1). Top view measures were: mesosoma length, mesosoma width, mesosoma segment number, petiole length, petiole width, postpetiole length, and postpetiole width. Head view measures were: head length, head width. To produce a size-matched dataset, we excluded the largest QLMs and smallest WTs until the means of the population were not significantly different, resulting in exclusion of the 7 smallest WTs and 8 largest QLMs. All morphometric analyses were performed and reported using both the full dataset and the size-matched dataset.

Principal components analysis was conducted in Prism 7 using a normalized dataset that combines our measurements with published measurements of *O. octoantenna* and *O. siamensis*.[1,2] To enable cross-species comparisons, normalization was achieved by linearly scaling each trait in each species to range from zero to one (Data S2C).

Foraging behavior

For behavior and fitness datasets, particular care was taken to specifically measure the effect of genotype (QLM versus WT) while controlling for age and rearing environment. Colonies used for experimental treatments were always matched to control for cohort variation among the chaperone ants.

Foraging experiments were conducted as reported previously.[39] Briefly, ants were maintained in a two-part dish with a 2cm diameter nest connected by a narrow opening to a 6.5cm diameter foraging arena. Ants were placed in the nest (with the opening to the foraging arena sealed) without brood and allowed to lay eggs. Once these eggs hatched into larvae (approximately 14 days later), the

Please cite this article in press as: Trible et al., A caste differentiation mutant elucidates the evolution of socially parasitic ants, Current Biology (2023), https://doi.org/10.1016/j.cub.2023.01.067

seal was removed to allow foragers to leave the nest, and food was placed in the foraging arena. Videos of foraging behavior and subsequent food retrieval were recorded and manually annotated as reported previously.[39] Colonies were fed, watered, and used for behavioral recordings every day until the larvae entered the prepupal stage (approximately 14 days after initiating recordings). This yielded approximately 10-15 foraging raids per colony. Small numbers of ants that died during the course of the experiment were removed the following day.

All behavioral experiments consisted of colonies established using 16 ants that were painted with color tags to make it easier to identify their genotype in the video recordings. Ant colonies were established using a strict paired design, such that every group of QLM ants was paired to a group of WT ants that was produced by the same rearing unit and subsequently reared in an identical manner. Ants ranged from 14 days to 2 months old at the start of experiments, and ages were matched within each pair. Pure colonies were all QLM (n = 4) or WT (n = 4). Mixed colonies (n = 8) were established with 8 QLMs and 8 WTs.

Fitness measurements

Egg-laying rates were measured from five replicate QLM and WT colonies that were matched for age, colony size, and rearing environment. Egg to pupa survival and eclosion survival were measured by establishing colonies with WT chaperones and varying proportions of QLM and WT brood.

Efficiency of larval rearing was measured using colonies with 20 WT or QLM chaperones established with <24h old eggs. When these eggs hatched into larvae, colonies were reduced to 16 first-instar larvae. Developmental transitions were scored as the date that the majority of surviving individuals had entered the respective developmental stage (L4: 4th larval instar;PP: prepupal stage; P:pupal stage, and Adult:eclosion). Overall survival from larva to adult was scored at the end of the experiment.

Whole-genome sequencing (Illumina)

17 DNA libraries were used for whole-genome Illumina sequencing. Tissues from individual adult ants were disrupted in a tissue lyser and genomic DNA was extracted using Qiagen's QIAmp DNA Micro Kit following manufacturer's recommendations. Libraries were prepared using Nextera Flex. Paired-end 150 base pair reads were sequenced on an Illumina NovaSeq SP Flow Cell. We aimed for 35X coverage to ensure sufficient read depth to accurately detect heterozygosity across the genome (Data S3A).

Short read data were processed following the GATK best practices pipeline[83] using the Obir v5.6 genome assembly generated in this study. Briefly, raw reads were trimmed with Trimmomatic 0.36,[70] aligned using BWA-MEM,[84] and sorted and de-duplicated before variants were called using HaplotypeCaller.[83]

Read depth distributions can contain excessively high and low values due to errors in genome assembly. These values can augment or diminish estimates of mean read depth across genomic regions. To avoid these effects, read depth was calculated using samtools depth[69] at stringently filtered SNPs. In addition to the standard GATK-recommended filtration steps, SNPs with null genotype calls, and SNPs with one or more samples having read depth greater than or equal to 80 (double the median read depth) were removed from the dataset. Because read depth differs among samples due to minor differences in library concentration during loading onto the Illumina flow cell, the normalized read depth was calculated by dividing the read depth at each SNP by the median read depth across all SNPs. Next, the mean normalized read depth was calculated for SNPs within each contig.

For molecular phylogenetics, whole-genome SNP calls (excluding sites with missing data in any library) were converted from vcf to fasta using vcf2phylip (https://github.com/edgardomortiz/vcf2phylip), such that heterozygous sites were represented using IUPAC uncertainty codes. These files were then used to create a diploid-aware phylogeny with the -GENOTYPE setting in RAxML-NG.[71,72] RAxML[72] was then used to estimate bootstrap support using the model -GTGTR4+G with 100 replicates.

Sites that distinguished the QLMs were defined as sites where both QLM libraries had the same genotype and differed from all 15 WT libraries. These sites were identified using a custom R script (https://github.com/bucktrible/qlm).

Improved genome assembly

To improve the assembly of Chromosome 13, we re-analyzed published data using the Falcon pipeline. First, we ran Falcon-unzip[73] using published PacBio data,[45] yielding primary (212Mbp, 322 contigs with N50 of 2.2Mbp) and alternate (67.8Mbp, 2685 contigs with N50 of 27.37kbp) assemblies. These assemblies were phased with published Hi-C data[45] using Falcon-phase,[74] and then scaffolded using the Obir v5.4 genome assembly using RaGOO.[75] Finally, this primary assembly, which we refer to as the Obir v5.6 assembly, was polished and masked as described previously.[45]

Next, we performed high molecular weight extractions of *O. biroi* following a published protocol[85] and sequenced two barcoded libraries using the Oxford Nanopore PromethION platform. Raw reads were assembled *de novo* using Flye (version 2.8.2)[86] and aligned to the Obir v5.6 contigs using Mauve (snapshot 2015-02-25).[77] This allowed us to manually re-order and re-orient the contigs of v5.6 by aligning them with the contigs of the two *de novo* assemblies as well as the Obir v5.4 assembly, yielding an improved Obir v5.7 assembly. Assemblies v5.6 and v5.7 do not differ in sequence content, but only in the position and orientation of Chromosome 13 contigs (see Data S3C).

Characterization of Chromosome 13

To document transposable element (TE) content in *O. biroi* and other species, we used RepeatModeler[78] and RepeatMasker[79] (https://repeatmasker.org/) to identify TEs belonging to known transposon classes from published genome assemblies (*O. biroi*: NCBI:GCA_003672135.1; *S. invicta*: NCBI:GCA_010367695.1; *D. melanogaster*: NCBI:GCA_000001215.4). To quantify gene

Please cite this article in press as: Trible et al., A caste differentiation mutant elucidates the evolution of socially parasitic ants, Current Biology (2023), https://doi.org/10.1016/j.cub.2023.01.067

content, we used the entire set of exons from the NCBI annotation of Obir v5.4 as a proxy (https://www.ncbi.nlm.nih.gov/genome/annotation_euk/Ooceraea_biroi/100/). We excluded predicted TE sequences that overlapped with annotated exons and exonic sequences that overlapped with predicted TEs from the analyses. We calculated the proportion of each scaffold comprised of each feature as the number of base pairs occupied by predicted TEs or annotated exons divided by the ungapped length of each scaffold in base pairs.

Gene-level analysis

To identify genes in the loss of heterozygosity region, we used the Mauve alignments (above) to identify contigs in the v5.4 genome assembly that aligned to the loss of heterozygosity region. We then used the published NCBI *O. biroi* annotation v5.4[45] to identify genes within those contigs. Genes in the loss of heterozygosity region were then tested for GO and KEGG enrichment using a custom R script (https://github.com/bucktrible/qlm).

O. biroi CYP9 genes were initially identified using a BLAST search using an exemplar protein (*O. biroi CYP9_1_1*). These results were then curated using the NCBI genome browser and amino acid sequence alignments to ensure that each gene name refers to a single enzyme. Every gene we report here is transcribed and contains intact CYP functional domains, implying that they are not pseudogenes. However, some *CYP9* genes lack start codons and may be transcribed and translated with their 5' neighbor. The spatial array of *CYP9* genes was created in Adobe Illustrator using start and stop coordinates of each exon. The phylogeny of *CYP9* genes was generated using RAxML. This phylogeny was also used to identify and remove proteins annotated as *CYP9s* that actually belong to the *CYP6* subfamily.

To quantify *CYP9* conservation and expansion, we obtained published CYP9 amino acid sequences from *Apis mellifera* and *Nasonia vitripennis*,[52] and the procedure described above was repeated for CYP9 proteins in three additional ant species that possess high-quality genomes and span the ant phylogeny (:*Harpegnathos saltator* NCBI:Hsalv8.5, *Monomorium pharaonis* NCBI:ASM326058v2, and *Camponotus floridanus* NCBI:Cflov7.5). Ant CYP9 enzymes were identified using a BLAST search with *O. biroi* CYP9_1_1 against the genome of each of the four ant species. All identified sequences were downloaded, and duplicates and sequences that fall phylogenetically outside of the insect CYP9 clade (as defined previously[52]) were removed. Note that 12 *CYP9* genes occur in the loss of heterozygosity region according to the Obir v5.4 genome assembly and annotation, but manual re-annotation of this assembly identified 24 *CYP9* genes in this region (Data S3F). Amino acid sequences are available at https://github.com/bucktrible/qlm.

QUANTIFICATION AND STATISTICAL ANALYSIS

Statistical analyses were performed using Graphpad's Prism 7, unless otherwise stated, and the details of statistical tests can be found in the figure legends. Code and packages used for genomics analyses are reported in data and software availability and method details.

Current Biology, Volume *33*

Supplemental Information

A caste differentiation mutant elucidates the evolution of socially parasitic ants

Waring Trible, Vikram Chandra, Kip D. Lacy, Gina Limón, Sean K. McKenzie, Leonora Olivos-Cisneros, Samuel V. Arsenault, and Daniel J.C. Kronauer

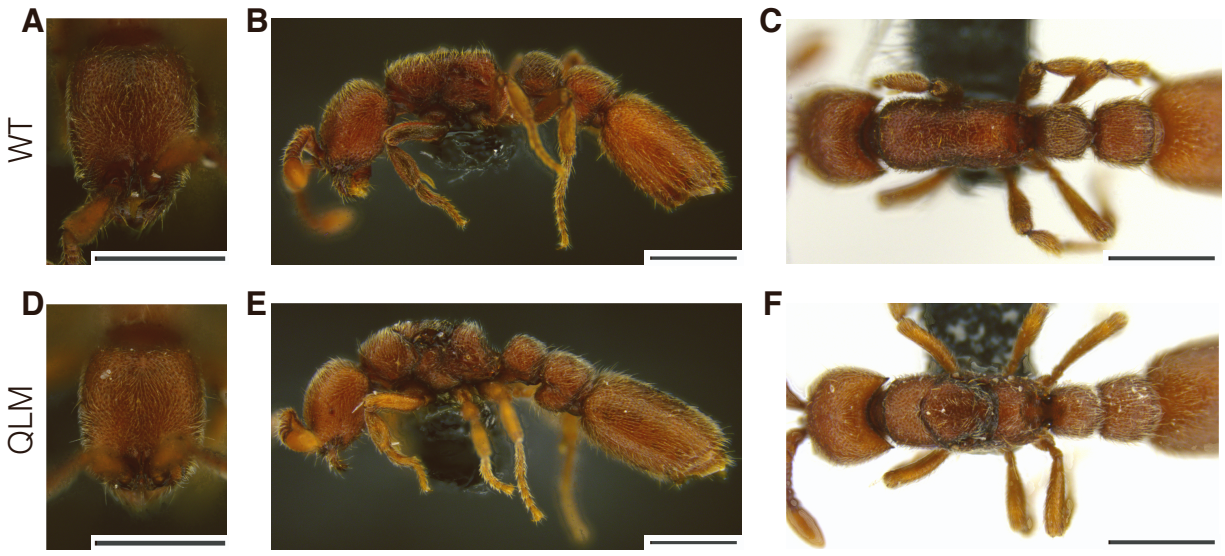

Figure S1. WT and QLM images, related to Figures 2 and 3. (A) and (D) WT and QLM head frontal view. (B) and (E) WT and QLM side view. Gaster tips were removed for ovariole dissections. (C) and (F) WT and QLM top view. Scale bars in (A-F): 0.5mm.

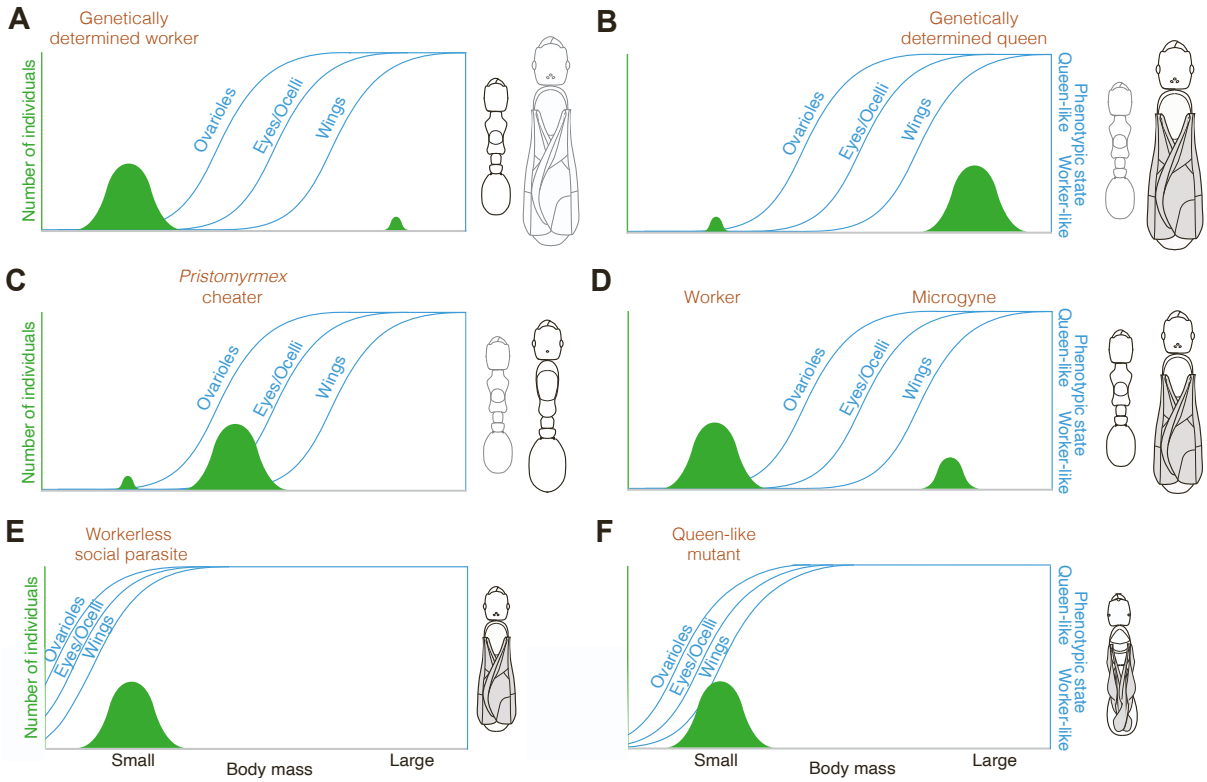

Figure S2. Cartoons and caste reaction norms for genetic variation in ant caste development, related to Figures 2 and 3. (A) Genetic bias for worker determination. Genetic biases for worker development are associated with thelytokous parthenogenesis of reproductive workers, as in *Ooceraea biroi* and *Pristomyrmex punctata*. Species with social hybridogenesis, such as *Wasmannia auropunctata* and *Cataglyphis mauritanica*, display genetic biases for worker development in certain genotypes and queen development in other genotypes[S1–S5]. These genetic systems act by increasing the probability that a larva will develop into a worker (potentially up to 100%) and can be interpreted as a genetic bias to body size that indirectly affects caste morphology[S2,S6,S7]. There is no evidence that genetic caste determination systems alter the mechanisms of caste differentiation or allometric scaling. *O. biroi* workers are morphologically comparable to those of related species (Figure 3) and, while winged queens have never been observed, large individuals have partially queen-like traits, indicating that the clonal raider ant displays a genetic bias for worker determination[S8]. (B) Genetic biases for queen determination are primarily documented from species with social hybridogenesis, which display genetic biases for worker development in certain genotypes and queen development in other genotypes. Most workerless social parasites display miniaturized queens that differ in allometric scaling relative to their closest free-living relatives (see panel E), but some large-bodied workerless social parasites may effectively represent genetically determined queens[S9–S11]. (C) Reproductive cheater genotype of *Pristomyrmex punctata*[S2]. Like in *O. biroi*, most clonal lines of *Pristomyrmex punctata* display a genetic bias for worker determination (A), but this divergent lineage shows a wingless queen phenotype: an increase in body size with partially queen-like ovaries, eyes, and mesosoma. Multiple free-living sexual *Pristomyrmex* species possess wingless queens with the same morphological syndrome as these cheaters, and rare small individuals of this cheater genotype display typical worker morphology, so we can conclude that this phenotype arose via a genetic bias toward larger body size, analogous to (B)[S12,S13]. Furthermore, these

cheaters do not morphologically resemble workerless social parasites and, unlike the *O. biroi* QLMs, they belong to their own clonal line, so it is not possible to infer the genetic architecture for social parasitism in this case. (D) Microgynes. Many facultatively parasitic species retain phenotypic plasticity for worker and queen development but have evolved microgynes, i.e., queens that are smaller than the typical queens of their genus. Unlike QLMs and workerless social parasites, microgynes appear to be equal to or larger in size than workers[S7,S14–S16]. Therefore, the evolution of microgynes represents a reduction in the size dimorphism between workers and queens, but there is no evidence that it entails an induction of queen-like morphology at worker-like body size. Recent phylogenetic and comparative evidence has failed to support the hypothesis that species with facultatively parasitic microgynes – or other forms of facultative social parasites – represent the evolutionary intermediates between free-living ants and workerless social parasites[S9,S17]. Instead, the closest relatives of most workerless social parasites appear to be free-living ants with phenotypically normal queens. (E) Workerless species with worker-sized queens. Every described species with this combination of morphological traits is an obligate inquiline (i.e., a workerless social parasite). Some of these workerless social parasites can produce rare worker offspring but, unlike in (B-D), these workers are morphologically abnormal and have extremely small body size[S18–S20]. Therefore, these workerless social parasites display a genetic change to the allometric scaling mechanisms of caste differentiation[S6]. This observation implies that, as in *O. biroi* QLMs, genetic lineages with worker-sized queens have workers that are reduced or absent. The only documented exception to this trend is the *Formica difficilis* species group, which has worker-sized queens and retains regular workers[S14,S17]. (F) *O. biroi* QLMs. To our knowledge, the QLMs represent the only documented intraspecific variant that lacks workers and displays queen-like morphology at worker-like body size in an ant. Like workerless social parasites (E), the QLMs display a change to allometric scaling. No such change has been demonstrated for genetically determined queens (B), *Pristomyrmex* cheaters (C), or microgynes (D). Note that, relative to typical *Ooceraea* queens (Figure 3), the morphology of the QLMs is uncoordinated: the wings do not inflate following eclosion and QLMs have only partially queen-like eyes and ocelli. This unusual combination of morphological features provides further evidence that the QLMs display a radical alteration to the allometric scaling mechanisms of caste differentiation.

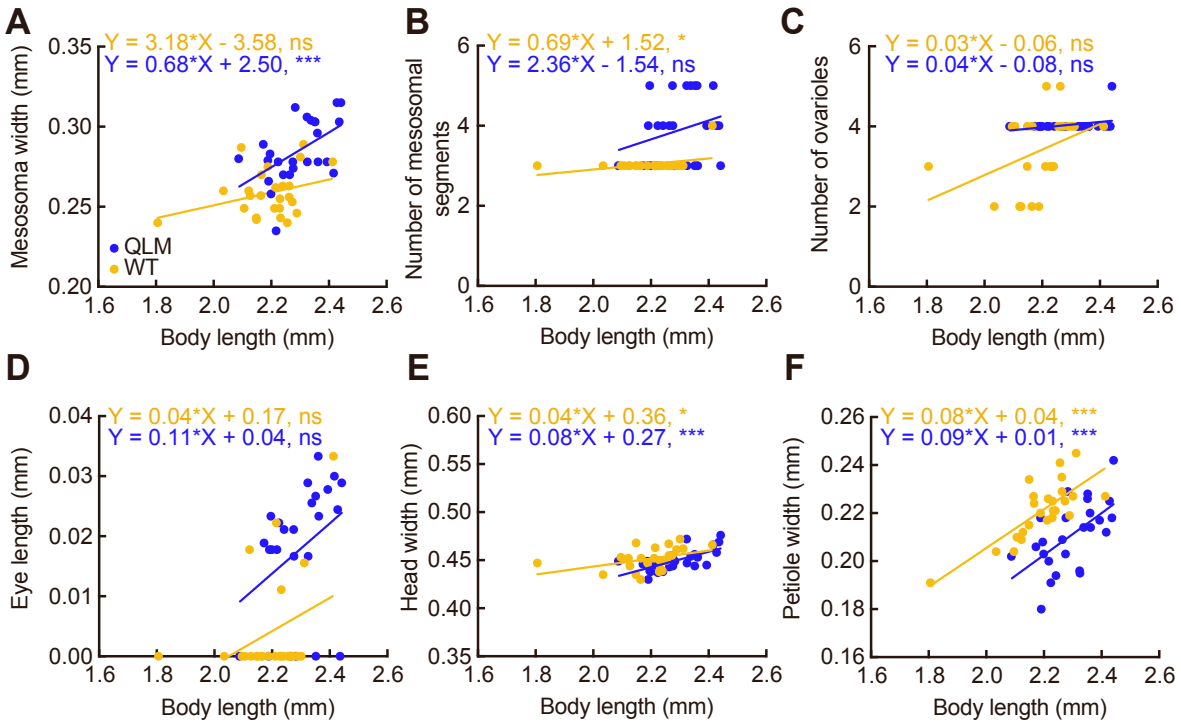

Figure S3. Supplementary WT and QLM morphometrics, related to Figures 2 and 3. (A) Mesosomal width. (B) Number of mesosomal segments. Three segments are characteristic of worker ants, while five segments are characteristic of queen ants. (C) Number of ovarioles. (D) Maximal length of pigmented photoreceptor patch of the eye. Values of 0 indicate none visible. (E) Head width. (F) Petiole width. All graphs depict n = 25 WT and QLM adults. ns: not significant; *p<0.05; ***p<0.001. p values from linear regression (Dfd = 23) with an expected slope of zero. Equations provide best-fit slope and y-intercept.

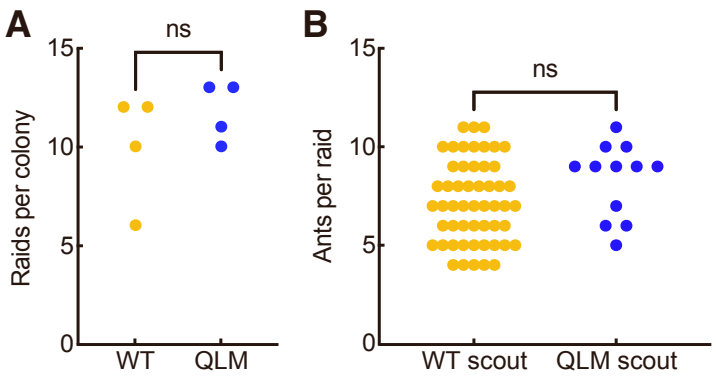

Figure S4. **Equal number and size of raids in WTs and QLMs, related to Figure 4.** (A) Raids per colony in 100% WT (n = 4) and 100% QLM (n = 4) colonies. QLM colonies do not engage in fewer raids than WT colonies. (B) Ants participating in raids initiated by WT or QLM scouts in mixed colonies (n = 66 raids). QLM scouts do not recruit fewer ants per raid than WT scouts.

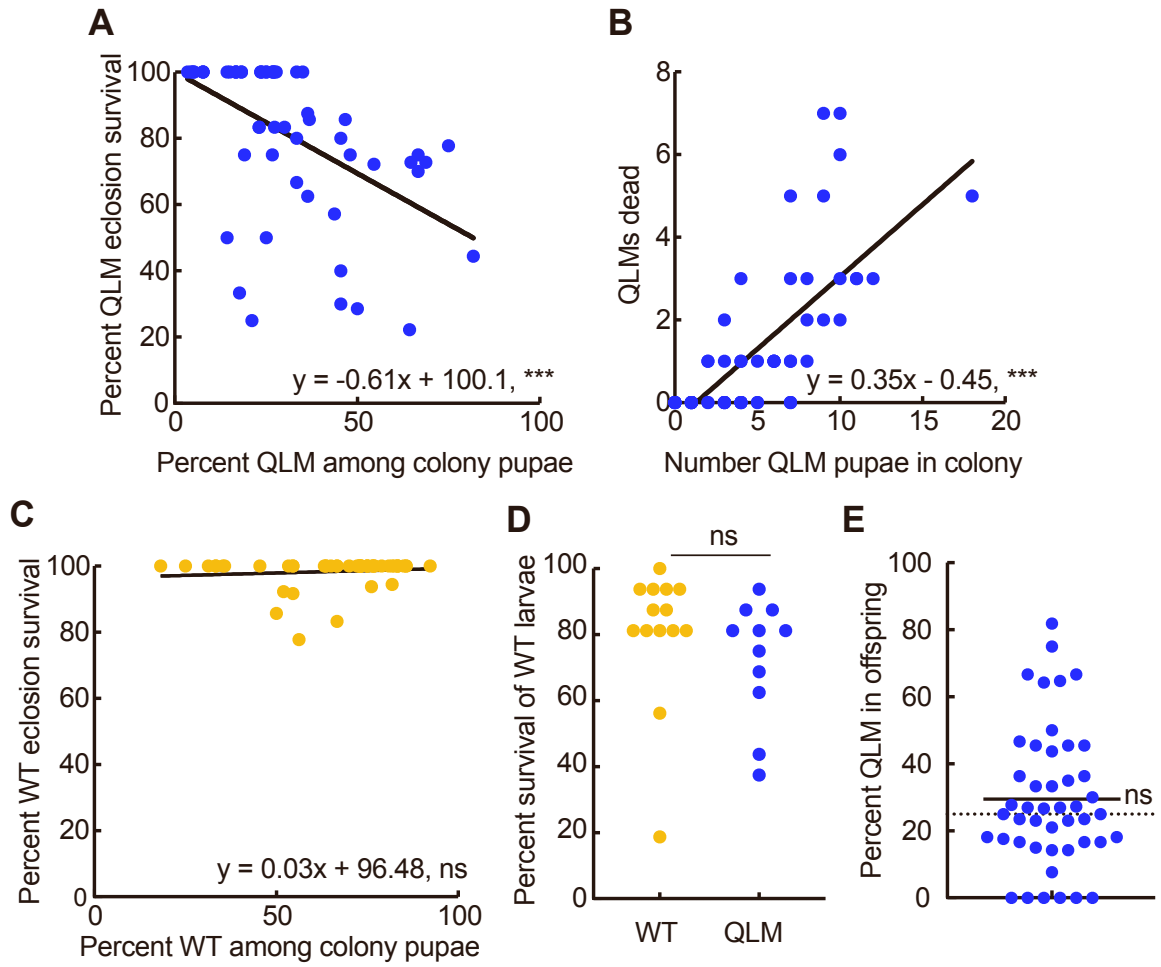

Figure S5. **QLMs show frequency-dependent survival as pupae, but rear larvae efficiently and persist at stable frequencies, related to Figure 5.** (A) Survival during eclosion for QLM pupae as a function of the percent of QLM pupae within the colony. (B) Number of QLM pupae that died during eclosion as a function of the number of QLM pupae within the colony. (C) Survival of WT pupae as a function of the percent of WT pupae within the colony. (D) Percent survival of WT larvae that were reared by WT or QLM adults. (E) Percent of QLM adults produced by colonies with 5 QLM and 15 WT adults. Percent of QLM adults produced was not significantly different from the percent of QLM adults in the colony (25%), implying that the frequency of QLM adults can remain approximately stable across generations. p values in (A-C) from linear regression with an expected slope of zero. Equations provide best-fit slope and y-intercept. p value in D from unpaired t-test, and p value in E from one-way Wilcoxon test. ns: not significant, ***p<0.001.

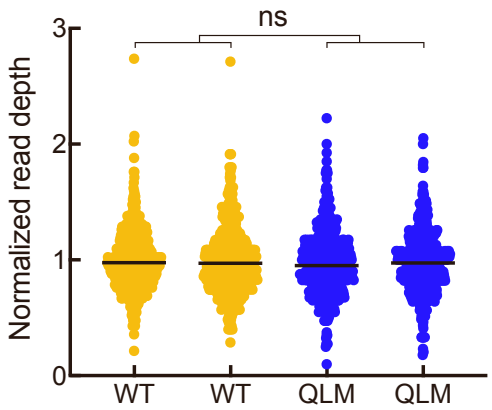

Figure S6. **Normalized read depth at Chromosome 13 loci, related to Figure 6.** QLMs do not differ from WTs in read depth at the loss of heterozygosity loci on Chromosome 13, indicating that the homozygous interval on Chromosome 13 represents a loss of heterozygosity rather than a deletion. ns: not significant. p value from paired t-test comparing WT and QLM average at each locus.

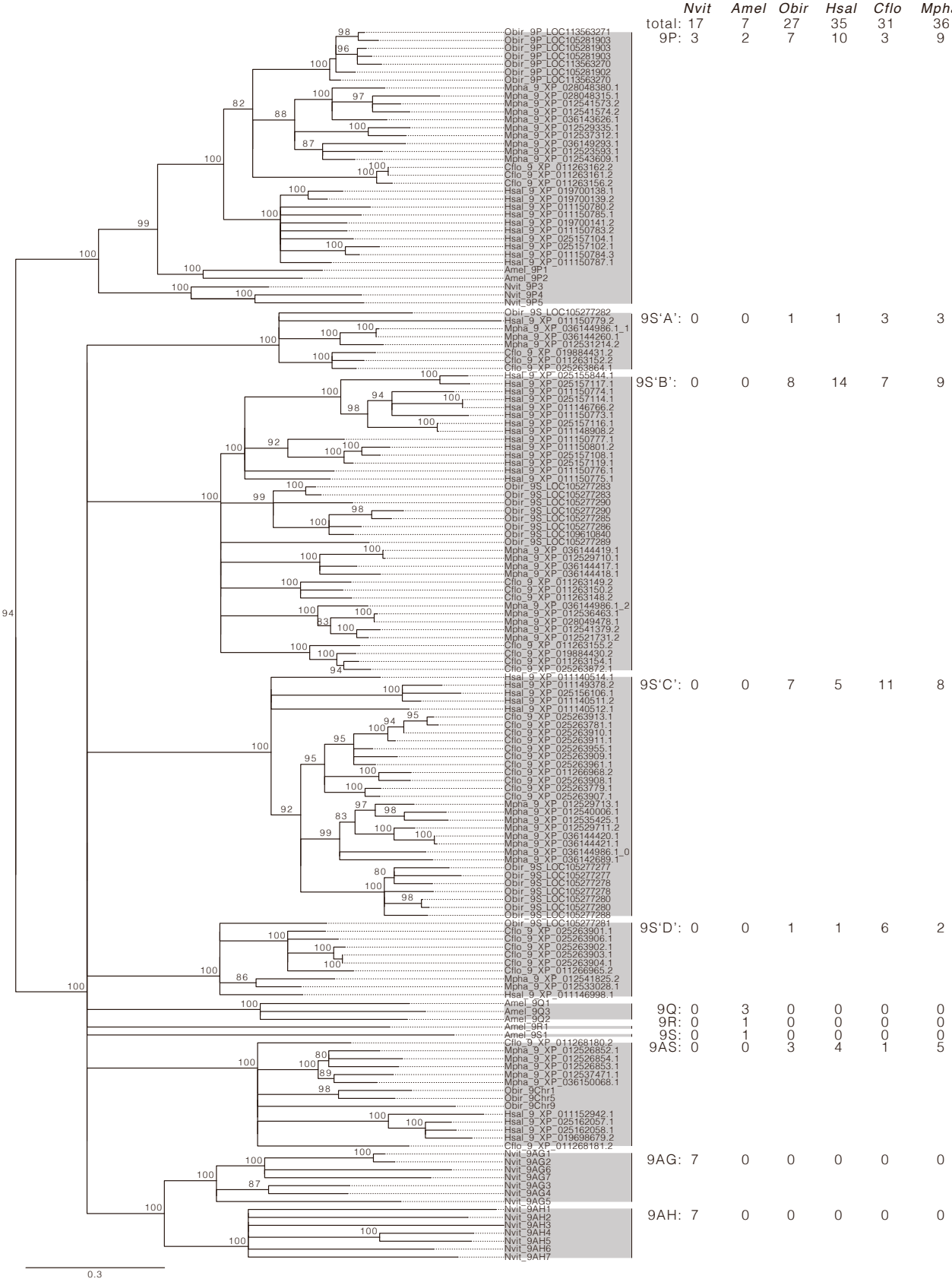
Nvit Amel Obir Hsal Cflo Mpha
total: 17 7 27 35 31 36
9P: 3 2 7 10 3 9
9S'A': 0 0 1 1 3 3
9S'B': 0 0 8 14 7 9
9S'C': 0 0 7 5 11 8
9S'D': 0 0 1 1 6 2
9Q: 0 3 0 0 0 0
9R: 0 1 0 0 0 0
9S: 0 1 0 0 0 0
9AS: 0 0 3 4 1 5
9AG: 7 0 0 0 0 0
9AH: 7 0 0 0 0 0
0.3

Figure S7. **Maximum likelihood phylogeny of CYP9 protein sequences derived from hymenopteran genomes, related to Figure 7.** Amel: *Apis mellifera*, Nvit: *Nasonia vitripennis*, Obir: *Ooceraea biroi*, Hsal: *Harpegnathos saltator*, Cflo: *Camponotus floridanus*, Mpha: *Monomorium pharaonis*. Each ortholog group is highlighted, and the numbers to the right give the number of copies in each species. All Chromosome 13 *CYP9*s in *O. biroi* fall within the loss of heterozygosity region and span five ortholog groups (CYP9P, CYP9S 'A'-'D'). All duplicate members of each CYP9 family are monophyletic in *O. biroi* as well as other ant species, and the *O. biroi* genes have a phylogeny concordant with their spatial organization (Figure 7B), indicating that a combination of gene conversion, duplication and deletion, and/or purifying selection has prevented the members of each ortholog group from diverging in sequence, resulting in a pattern of coordinated evolution. Node labels represent bootstrap support from 100 replicates, and the scale bar represents 30% divergence at informative sites. Nodes with less than 80% bootstrap support were collapsed.

Clonal Line	Colonies	Individuals	Microsatellite locus					
			DK371	ES177	D8Z0W	D8M16	D4XW2	ER4IH
Line A	19	27	192/192	219/219	231/231	180/188	214/220	227/227
Line A	4	5	192/192	219/219	231/231	180/188	220/220	227/227
Line B	31	31	192/192	216/219	231/233	180/182	217/220	227/230
Line B	9	9	192/192	219/219	231/233	180/182	217/220	227/230
Line B	3	3	192/192	216/216	231/233	180/182	217/220	227/230
Line B	2	2	192/192	216/219	231/231	180/182	220/220	227/230
Line B	1	1	192/192	216/216	231/233	180/182	217/220	227/227
Line B	1	1	186/192	219/221	229/231	176/180	214/220	227/230
Line B	1	1	186/192	219/221	229/231	176/180	214/220	227/227
Line C	8	8	186/192	213/213	229/231	176/199	214/214	236/236
Line D	1	1	186/186	213/213	231/231	176/197	214/220	227/236
Line D	1	1	192/192	219/219	231/231	176/197	214/220	227/236
Queen-like mutant	1	6	192/192	219/219	231/231	180/188	214/220	227/227
Queen-like mutant	1	1	192/192	219/219	231/231	180/188	214/214	227/227

Table S1. Microsatellite genotypes for queen-like mutants and the four invasive clonal lines of *O. biroi*, related to Figure 1. Queen-like mutants belong to Clonal Line A and, like wild-types, are parthenogenetic.

Supplementary References

S1. Connallon, T., and Hodgins, K.A. (2021). Allen Orr and the genetics of adaptation. Evolution *75*, 2624–2640.

S2. Kuhn, A., Darras, H., and Aron, S. (2018). Phenotypic plasticity in an ant with strong caste – genotype association. Biol. Lett. *14*, 20170705.

S3. Oxley, P.R., Ji, L., Fetter-Pruneda, I., McKenzie, S.K., Li, C., Hu, H., Zhang, G., and Kronauer, D.J.C. (2014). The genome of the clonal raider ant *Cerapachys biroi*. Curr. Biol. *24*, 451–458.

S4. Dobata, S., Sasaki, T., Mori, H., Hasegawa, E., Shimada, M., and Tsuji, K. (2009). Cheater genotypes in the parthenogenetic ant *Pristomyrmex punctatus*. Proc. Biol. Sci. *276*, 567–574.

S5. Fournier, D., Estoup, A., Orivel, J., Foucaud, J., Jourdan, H., Le Breton, J., and Keller, L. (2005). Clonal reproduction by males and females in the little fire ant. Nature *435*, 1230–1234.

S6. Trible, W., and Kronauer, D.J.C. (2020). Hourglass model for developmental evolution of ant castes. Trends Ecol. Evol. *36*, 100–103.

S7. Trible, W., and Kronauer, D.J.C. (2017). Caste development and evolution in ants: it's all about size. J. Exp. Biol. *220*, 53–62.

S8. Ravary, F., and Jaisson, P. (2004). Absence of individual sterility in thelytokous colonies of the ant *Cerapachys biroi* Forel (Formicidae, Cerapachyinae). Insectes Soc. *51*, 67–73.

S9. Rabeling, C. (2021). Social Parasitism. Encycl. Soc. Insects, 836–858.

S10. Rabeling, C., Schultz, T.R., Pierce, N.E., and Bacci, M. (2014). A social parasite evolved reproductive isolation from its fungus-growing ant host in sympatry. Curr. Biol. *24*, 2047–2052.

S11. Schwander, T., Lo, N., Beekman, M., Oldroyd, B.P., and Keller, L. (2010). Nature versus nurture in social insect caste differentiation. Trends Ecol. Evol. *25*, 275–82.

S12. Tsuji, K., and Dobata, S. (2011). Social cancer and the biology of the clonal ant *Pristomyrmex punctatus* (Hymenoptera: Formicidae). Myrmecological News *15*, 91–99.

S13. Wang, M. (2003). A monographic revision of the ant genus *Pristomyrmex* (Hymenoptera: Formicidae). Bull. Museum Comp. Zool. *157*, 383–542.

S14. Trible, W., and Kronauer, D.J.C. (2021). Ant caste evo-devo: Size predicts caste (almost) perfectly. Trends Ecol. Evol. *36*, 671–673.

S15. McInnes, D.A., and Tschinkel, W.R. (1995). Queen dimorphism and reproductive strategies in the fire ant *Solenopsis geminata* (Hymenoptera: Formicidae). Behav. Ecol. Sociobiol. *36*, 367–375.

S16. Rüppell, O., Heinze, J., and Hölldobler, B. (1998). Size-dimorphism in the queens of the North American ant *Leptothorax rugatulus* (Emery). Insectes Soc. *45*, 67–77.

S17. Borowiec, M.L., Cover, S.P., and Rabeling, C. (2021). The evolution of social parasitism in *Formica* ants revealed by a global phylogeny. Proc. Natl. Acad. Sci. *118*, e2026029118.

S18. Wilson, E.O. (1984). Tropical social parasites in the ant genus *Pheidole*, with an analysis of the anatomical parasitic syndrome (Hymenoptera: Formicidae). Insectes Soc. *31*, 316–334.

S19. Cole, A.C. (1965). Discovery of the worker caste of *Pheidole* (P.) *inquilina*, new combination (Hymenoptera: Formicidae). Ann. Entomol. Soc. Am. *58*, 173–175.

S20. Sumner, S., Nash, D.R., and Boomsma, J.J. (2003). The adaptive significance of inquiline

parasite workers. Proc. Biol. Sci. *270*, 1315–1322.
S21. Yang, S., Wang, L., Huang, J., Zhang, X., Yuan, Y., Chen, J.Q., Hurst, L.D., and Tian, D. (2015). Parent-progeny sequencing indicates higher mutation rates in heterozygotes. Nature *523*, 463–467.
S22. Liu, H., Jia, Y., Sun, X., Tian, D., Hurst, L.D., and Yang, S. (2017). Direct determination of the mutation rate in the bumblebee reveals evidence for weak recombination-associated mutation and an approximate rate constancy in insects. Mol. Biol. Evol. *34*, 119–130.
S23. Dermauw, W., Van Leeuwen, T., and Feyereisen, R. (2020). Diversity and evolution of the P450 family in arthropods. Insect Biochem. Mol. Biol. *127*, 103490.
S24. Peeters, C., and Crozier, R.H. (1988). Caste and reproduction in ants: not all mated egg-layers are "queens." Psyche *95*, 283–288.
S25. Yagound, B., Dogantzis, K.A., Zayed, A., Lim, J., Broekhuyse, P., Remnant, E.J., Beekman, M., Allsopp, M.H., Aamidor, S.E., Dim, O., *et al.* (2020). A single gene causes thelytokous parthenogenesis, the defining feature of the Cape honeybee *Apis mellifera capensis*. Curr. Biol. *30*, 1–12.
S26. Fresneau, D., and Dupuy, P. (1988). A study of polyethism in a ponerine ant: *Neoponera apicalis* (Hymenoptera, Formicidae). Anim. Behav. *36*, 1389–1399.
S27. Glastad, K.M., Graham, R.J., Ju, L., Roessler, J., Brady, C.M., and Berger, S.L. (2020). Epigenetic regulator CoREST controls social behavior in ants. Mol. Cell *77*, 338-351.
S28. Rey, O., Facon, B., Foucaud, J., Loiseau, A., and Estoup, A. (2013). Androgenesis is a maternal trait in the invasive ant *Wasmannia auropunctata*. Proc. R. Soc. B Biol. Sci. *280*, 20131181.
S29. Lacy, K.D., Shoemaker, D., and Ross, K.G. (2019). Joint evolution of asexuality and queen number in an ant. Curr. Biol. *29*, 1394–1400.